HHS Public Access

Author manuscript

Neurobiol Aging. Author manuscript; available in PMC 2017 August 01.

Published in final edited form as:

Neurobiol Aging. 2016 August ; 44: 185–196. doi:10.1016/j.neurobiolaging.2016.04.019.

Comparative Pathobiology of Aβ and the Unique Susceptibility of Humans to Alzheimer's Disease

Rebecca F. Rosen[a,§], **Yasushi Tomidokoro**[b,¶], **Aaron S. Farberg**[a,⌘], **Jeromy Dooyema**[a], **Brian Ciliax**[c], **Todd M. Preuss**[a,d], **Thomas A. Neubert**[e], **Jorge A. Ghiso**[b], **Harry LeVine III**[f], and **Lary C. Walker**[a,c]

[a]Yerkes National Primate Research Center, Emory University, Atlanta, GA 30329, USA

[b]Departments of Pathology and Psychiatry, NYU School of Medicine, New York, NY 10016, USA

[c]Department of Neurology, Emory University School of Medicine, Atlanta, GA 30322, USA

[d]Department of Pathology and Laboratory Medicine, Emory University School of Medicine, Atlanta, GA, 30322, USA

[e]Department of Biochemistry and Molecular Pharmacology, and Kimmel Center for Biology and Medicine at the Skirball Institute, NYU School of Medicine, New York, NY 10016, USA

[f]Center on Aging, Center for Structural Biology, Department of Molecular & Cellular Biochemistry, University of Kentucky, Lexington, KY 40536, USA

Abstract

The misfolding and accumulation of the protein fragment Aβ is an early and essential event in the pathogenesis of Alzheimer's disease (AD). Despite close biological similarities among primates, humans appear to be uniquely susceptible to the profound neurodegeneration and dementia that characterize AD, even though nonhuman primates deposit copious Aβ in senile plaques and cerebral amyloid-β angiopathy as they grow old. Since the amino acid sequence of Aβ is identical in all primates studied to date, we asked whether differences in the properties of aggregated Aβ might underlie the vulnerability of humans and the resistance of other primates to AD. In a comparison of aged squirrel monkeys (*Saimiri sciureus*) and humans with AD, immunochemical and mass spectrometric analyses indicate that the populations of Aβ fragments are largely similar in the two species. In addition, Aβ-rich brain extracts from the brains of aged squirrel monkeys

Correspondence concerning this article should be addressed to: Rebecca F. Rosen, Center for Urban Science & Progress, New York University, Brooklyn, NY, 11201, USA, Phone number: 646-997-0529, rebecca.rosen@nyu.edu or Lary C. Walker, Yerkes National Primate Research Center, Emory University, Atlanta, GA, 30329, USA, Phone number: 404-727-7779, lary.walker@emory.edu.
[§]Current affiliation: Center for Urban Science & Progress, New York University, Brooklyn, NY 11201, USA
[⌘]Current affiliation: Clinical Research Fellow, National Society for Cutaneous Medicine, New York, NY
[¶]Current affiliation: Department of Neurology, University of Tsukuba, Tsukuba, Ibaraki 305-8577, Japan

7. Disclosure

The authors have no conflicts of interest to disclose.

8. Appendix

None

and AD patients similarly seed the deposition of Aβ in a transgenic mouse model. However, the epitope exposure of aggregated Aβ differs in SDS-stable oligomeric Aβ from the two species. In addition, the high-affinity binding of ^{3}H Pittsburgh Compound B (PiB) to Aβ is significantly diminished in tissue extracts from squirrel monkeys compared to AD patients. These findings support the hypothesis that differences in the pathobiology of aggregated Aβ among primates are linked to post-translational attributes of the misfolded protein, such as molecular conformation and/or the involvement of species-specific cofactors.

Keywords

Amyloid; cerebral amyloid angiopathy; primate; prion; seeding; tauopathy; senile plaques

1. Introduction

Genetic, pathologic, and biochemical evidence indicates that the aggregation of the β-amyloid peptide (Aβ) is a key factor in the pathogenesis of AD (Bateman, et al., 2012,Bilousova, et al., 2016,Hardy and Selkoe, 2002,Holtzman, et al., 2011,Nelson, et al., 2012). Aβ is an amphiphilic peptide, most often 40 or 42 amino acids in length, that is cleaved from the Aβ-precursor protein (APP); in AD, Aβ self-assembles into oligomers, protofibrils, and amyloid fibrils in the brain parenchyma and vasculature (Bitan, et al., 2005,Catalano, et al., 2006,Ferreira, et al., 2015,Hamley, 2012,Kuo, et al., 1996,Revesz, et al., 2003,Selkoe, 2011). The subsequent cascade of events includes the ectopic polymerization of tau in neurofibrillary tangles, loss of neurons and their connections, progressive cognitive decline, and death (Holtzman, et al., 2011,Querfurth and LaFerla, 2010).

Both Aβ deposition and tauopathy are necessary for the full phenotypic expression of AD (Bakota and Brandt, 2016,Nisbet, et al., 2015,Selkoe, 2011), and the number of neurofibrillary tangles correlates strongly with the degree of dementia (Arriagada, et al., 1992,Bierer, et al., 1995,Crystal, et al., 1988,Simic, et al., 2016). However, evidence from genetic, *in vivo* imaging and biochemical studies pinpoints the misfolding and aggregation of Aβ as the earliest critical event in the ontogeny of AD (Bateman, et al., 2012,Bilousova, et al., 2016,Holtzman, et al., 2011,Nelson, et al., 2012,Selkoe, 2011). Importantly, emerging analyses of Aβ and tau biomarkers indicate that the pathogenic cascade leading from Aβ accumulation to tauopathy and dementia begins in the brain more than a decade prior to the onset of clinical signs and symptoms (Bateman, et al., 2012,Buchhave, et al., 2012,Holtzman, et al., 2011,Jack and Holtzman, 2013,Sperling, et al., 2013).

Despite compelling evidence for a principal role of Aβ aggregation in AD, the accumulation of cerebral Aβ deposits *per se* is not always associated with frank dementia or neurodegeneration. Transgenic rodent models overproducing human-sequence Aβ develop profuse senile plaques and cerebral amyloid-β angiopathy (CAA), but they do not have substantial, AD-like neuronal cell loss, neurofibrillary tangles, and/or profound memory impairment (Jucker, 2010,Morrissette, et al., 2009). Aged nonhuman primates naturally accumulate abundant multimeric, human-sequence Aβ in plaques and CAA (D'Angelo, et

al., 2013,Elfenbein, et al., 2007,Gearing, et al., 1996,Gearing, et al., 1997,Geula, et al., 2002,Heuer, et al., 2012,Lemere, et al., 2004,Lemere, et al., 2008,Perez, et al., 2013,Selkoe, et al., 1987,Walker, et al., 1990), yet they appear to be resistant to other behavioral and pathologic features that define AD in humans (Finch and Austad, 2012,Finch and Austad, 2015,Heuer, et al., 2012,Walker and Cork, 1999). Similarly, dogs generate human-sequence Aβ and manifest senile plaques and CAA in old age, but they also do not exhibit all features of AD (Fast, et al., 2013,Head, 2013).

The paradoxical existence of extensive cerebral Aβ-amyloidosis without overt neurodegeneration and dementia in animal models (and possibly humans) might be reconciled by differences in the post-translational characteristics of Aβ, such as species-specific populations of Aβ isoforms or the formation of structurally and functionally distinct proteopathic ‘strains’ (Fritschi, et al., 2014,Hatami, et al., 2014,Heilbronner, et al., 2013,Levine and Walker, 2010,Lu, et al., 2013,Mehta, et al., 2013,Meyer-Luehmann, et al., 2006,Petkova, et al., 2005,Rosen, et al., 2010a,Rosen, et al., 2011,Stohr, et al., 2014,Watts, et al., 2014). To gain insight into the comparative pathobiology of Aβ in a species proximal to humans, we analyzed the properties of Aβ in the brains of humans with AD and aged squirrel monkeys (*Saimiri sciureus*), a New World primate that develops senile plaques and CAA with advancing age (Elfenbein, et al., 2007,Walker, et al., 1987,Walker, et al., 1990). We found that the populations of Aβ and its post-translationally variant isoforms are remarkably similar in humans and squirrel monkeys, and that Aβ-rich cortical extracts from aged squirrel monkeys effectively seed the deposition of Aβ in an APP-transgenic mouse model. However, a radioligand binding assay confirmed that high-affinity binding sites for the amyloid imaging agent Pittsburgh Compound B (PiB) are deficient in Aβ-rich brain extracts from aged monkeys compared to humans with AD (Rosen et al., 2011). Moreover, the epitope display of aggregated Aβ differs in SDS-stable oligomeric Aβ from the two species. In light of the absence of AD-like cognitive dysfunction in aged nonhuman primates (Heuer, et al., 2012,Walker and Cork, 1999), these findings indicate that differences in the post-translational characteristics of Aβ may govern the distinctive vulnerability of humans to Alzheimer's disease.

2. Methods

2.1. Subjects

Postmortem brain tissue was analyzed from 7 aged squirrel monkeys (*Saimiri sciureus*), 9 humans with end-stage AD, and 3 aged, nondemented humans (Table 1). These cases were part of a previous histological analysis of the binding of PiB in primates (Rosen, et al., 2011). The known maximum lifespan of squirrel monkeys is approximately 30 years (Chen, et al., 2013,Finch and Sapolsky, 1999,Herndon, et al., 1999,Herndon, et al., 1998). Squirrel monkey specimens were collected in accordance with federal and institutional guidelines for the humane care and use of experimental animals. Human tissues were obtained from the Emory University Alzheimer's Disease Research Center Brain Bank compliant with federal and institutional guidelines, and were coded to protect the anonymity of subjects.

The presenilin/APP (APP/PS1) transgenic mice used in the seeding experiment carried co-segregating transgenes for APPSwe and PSEN1dE9, driven by the prion protein (PrP)

promoter (Borchelt, et al., 1997). The mice were obtained from Jax labs (B6C3-Tg(APPswe,PSEN1dE9)85Dbo/J).

2.2. Tissue collection and preparation

For biochemical analyses, unfixed, fresh-frozen temporal (superior temporal gyrus) and occipital (pericalcarine) cortical tissue blocks were weighed and Dounce-homogenized in 5 volumes of homogenization buffer (50mM Tris-HCl /150mM NaCl, pH 7.5, containing complete protease inhibitor [Santa Cruz Biochemicals, Santa Cruz, CA, USA]). Homogenates were centrifuged at 100,000×*g* for 60 minutes at 4°C in a TLA 100.4 rotor (Beckman Coulter, Fullerton, CA, USA), and the supernatant ("soluble extract" containing primarily oligomeric and/or monomeric Aβ) was aliquoted and stored at –80°C until use. The underlying buffer-insoluble pellet was probe-sonicated with a microtip sonicator (Sonic Dismembrator 100, Fisher Scientific, Waltham, MA, USA) at Level 4 for 30 seconds in 70% formic acid (Sigma-Aldrich), centrifuged at 16,110×*g* for 60 minutes at 4°C, and the supernatant ("insoluble extract") aliquoted and stored at –80°C until use.

To prepare clarified tissue extracts for seeding injections, SDS-PAGE, and autoradiographic analysis (see below), unfixed, fresh-frozen temporal and occipital cortical tissue blocks were weighed and Dounce-homogenized in 4 volumes of sterile, ice-cold, 0.1M phosphate-buffered-saline (PBS), pH 7.4. These 20% (w/v) homogenates were sonicated with the microtip sonicator at Level 4 for 3 × 5 seconds, vortexed, centrifuged for 5 minutes at 3,000×*g*, and the clear supernatants (extracts) stored at –80°C until use (Kane, et al., 2000,Meyer-Luehmann, et al., 2006,Rosen, et al., 2010b,Walker, et al., 2002).

For immunohistochemical analysis of fixed tissue, specimens were immersion-fixed for at least 7 days in PBS-buffered, de-polymerized 4% paraformaldehyde. Temporal and occipital blocks were transversely bisected so that both fixed-frozen and paraffin sections could be taken from the same general region. For the fixed-frozen sections, tissue blocks were cryoprotected in a graded series of 10%-30% sucrose, embedded in Tissue-Tek OCT mounting medium (Sakura, Torrance CA), frozen, and then sectioned at 50μm thickness on a cryostat at –20°C. Sections were stored in antifreeze (30% ethylene glycol in 30% sucrose/PBS) at –20°C until use. The remaining blocks were paraffin-embedded, sectioned at 8μm thickness and mounted onto silanized slides.

2.3. Antibodies

The following antibodies were used for immunohistochemistry, immunoprecipitation, and/or immunoblotting: Monoclonal antibodies 6E10 and 4G8 generated to residue segments 1-16 and 17-24 of the Aβ peptide, respectively (Covance Research Products, Denver, PA, USA); rabbit polyclonal antibodies R361 and R398 specific to C-terminal residues of Aβ40 and Aβ42, respectively (kindly provided by Dr. Pankaj Mehta, Institute for Basic Research on Developmental Disabilities, Staten Island, NY, USA); monoclonal antibody 8E1 to Aβ[pE3]-x (IBL Japan, Gunma, Japan); monoclonal antibodies CP13 to phospho-tau 202, PHF1 to phospho-tau 396/404, or MC1 to a conformational epitope on aggregated tau (all courtesy of Dr. Peter Davies, Feinstein Institute for Medical Research, Manhasset, NY, USA); and

monoclonal antibody AT8 to phospho-tau 202/205 (Covance) (Rosen, et al., 2008,Rosen, et al., 2011).

2.4. Immunohistochemistry

To prepare slide-mounted paraffin sections for immunohistochemistry, sections were de-paraffinized by heating in an oven for 30 minutes at 60°C followed by 1 minute incubations in xylene, 100% ethanol, 95% ethanol, 70% ethanol, and de-ionized water. Paraffin-embedded and frozen (50 μm-thick floating) sections were washed in 0.1M PBS, pH 7.4, and endogenous peroxidases inactivated with 3% H_2O_2 in methanol. To inhibit nonspecific reagent binding, sections were incubated in a blocking solution consisting of 2% normal serum (horse serum for monoclonal antibodies and goat serum for polyclonal antibodies) and 0.2% Tween-20 (Sigma-Aldrich, St. Louis, MO) in PBS for one hour at room temperature. To enhance Aβ-immunodetection, sections were pretreated for 10 minutes with 100% formic acid. They were next placed in blocking solution, then incubated in primary antibody (diluted in blocking solution) for one hour at room temperature and then overnight at 4°C. On the second day, Vectastain Elite kits (Vector Laboratories, Burlingame, CA, USA) were used for avidin-biotin complex (ABC)-based horseradish peroxidase immunodetection of antigen-antibody complexes. After rinsing, sections were placed for one hour at room temperature in biotinylated secondary antibody (1:200 in blocking solution). They were then rinsed, immersed for 30 minutes in avidin-biotin-peroxidase complex, developed with 3,3'-diaminobenzidine (DAB) (Vector Laboratories), and mounted onto glass slides. Tissue from pathologically verified human AD cases was used as positive control material for immunohistochemistry, and non-immune mouse IgG or rabbit serum was used in place of the primary antibodies as negative controls. Images were recorded with a Leica DMLB microscope (Leica, Wetzlar, Germany) and Spot Flex digital camera (Diagnostic Instruments, Sterling Heights, MI).

2.5. ELISA quantitation of Aβ levels

Soluble cortical Aβx-40 and Aβx-42 levels were quantified in TBS extracts using 96-well microplates coated with a C-terminal-specific capture antibody and an N-terminal-specific detection antibody, according to the manufacturer's instructions (The Genetics Company, Schlieren, Switzerland). After stopping the tetramethylbenzidine-peroxidase reaction with sulfuric acid, plates were read at 450 nm on a Biotek Synergy HT Multidetection plate reader (Biotek, Winooski, VT, USA). All samples were assayed in duplicate and the Aβ content expressed relative to the wet weight of tissue. Insoluble Aβ was quantified using the same methodology after formic acid extracts were neutralized and diluted, as previously described (Rosen, et al., 2011).

2.6. MALDI-TOF mass spectrometry

To compare the Aβ fragments present in AD cases and aged squirrel monkeys, Aβ peptides in soluble and insoluble extracts from the temporal and occipital cortices were analyzed by matrix-assisted laser desorption/ionization-time of flight mass spectrometry (MALDI-TOF MS) in 3-6 subjects from each of the 3 experimental groups (AD: temporal cortex, n=3; occipital cortex, n=6; nondemented humans (ND): temporal cortex, n=3; Squirrel monkeys: temporal cortex, n=3, occipital cortex, n=4).

Total Aβ was immunoprecipitated from cortical extracts and analyzed by western blot and MALDI-TOF MS as previously described (Tomidokoro, et al., 2005). Briefly, 50μl of Dynal M-280 Dynabeads (Invitrogen, Carlsbad, CA) coated with sheep anti-mouse antibodies were incubated for 24 hours at 4°C with monoclonal antibodies 4G8 and 6E10, each at a concentration of 60μg/ml (3μg of each antibody/50μl beads) while rotating end-over-end. Nonspecific binding sites on antibody-coated beads were blocked with 0.1% bovine serum albumin (Sigma-Aldrich, St. Louis, MO). To minimize nonspecific binding to the beads, the extracts were first "cleared" by incubation with uncoated beads. Accordingly, 25μl of uncoated beads were added to 1.0ml of each soluble cortical extract or to each solution of 100μl formic acid-treated extract that had been neutralized with 1.0M Tris to pH 7.4 and diluted up to 10ml with deionized water. Samples and beads were incubated, rotating end-over-end, for one hour at room temperature. For each immunoprecipitation (IP) reaction, 50μl of Aβ antibody-coated beads were added to the cleared extracts and incubated, rotating, for 3 hours at room temperature followed by 12 hours at 4°C. As a negative control, beads with no antibodies were incubated with cortical extracts from each group. Synthetic Aβ40 incubated with antibody-coated beads served as a positive control. In all cases, beads were subsequently washed 3 times in ice-cold PBS and once in 50 mM ammonium bicarbonate (pH 7.3), followed by elution in 0.5% formic acid. The eluted material was dried down in a Savant Speed Vac concentrator (Thermo Fisher) and further reconstituted in 4μl of 0.1% formic acid in 20% acetonitrile. One fourth of the reconstituted sample (1μl) was combined with an equal volume of α-cyano-4-hydroxycinnamic acid matrix (Agilent Technologies) reconstituted in 0.1% trifluoroacetic acid and 100% acetonitrile at a concentration of 15 g/L and 1 μl of the resulting mixture analyzed in a Micromass Tof-Spec-2E MALDI-TOF mass spectrometer in linear mode and standard instrument settings. External mass calibration was performed using human adrenocorticotropic hormone peptide 18–39 (average mass = 2465.68 Da) and insulin (average mass = 5733.49 Da) as standards. In all cases, MS spectra were processed and analyzed by FlexAnalysis and major peaks within the spectra identified with ExPASy's FindPept software (http://us.expasy.org/tools/findpept.html). Peaks that were detected in the negative control (mock immunoprecipitation with no antibodies) were not included in the final analysis.

2.7. Western blot analysis

To investigate differences in the pattern of Aβ aggregation between AD and aged squirrel monkey brain specimens, 60μg of total protein from cortical extracts – quantitated with bicinchoninic acid/cupric sulfate according to the manufacturer's instructions (Pierce BCA Protein Assay Kit, Thermo Scientific, Rockford, IL) – was incubated with 2x Tricine loading buffer in the presence of a reducing agent, boiled for 5 minutes and loaded onto a 10-20% Tris-Tricine gel (Invitrogen). SeeBlue 2 molecular marker (Invitrogen) and 100ng synthetic, pre-aggregated Aβ42 (rPeptide, Bogart, GA) were run on each gel as a molecular weight marker and positive control, respectively. Protein was transferred to nitrocellulose membranes that were then boiled for 15 minutes in 0.1M PBS before blocking for 30 minutes at room temperature in 2.5% milk in Tris-buffered saline with 0.05% Tween-20 (TBS-T). After a 30 minute rinse in TBS-T, membranes were incubated for one hour at room temperature and then 12 hours at 4°C with either 6E10 (1:1000) or 4G8 (1:2500) primary anti-Aβ antibodies diluted in 2.5% milk/TBS-T. On day 2, the membranes were rinsed for 30

minutes in TBS-T, incubated for 90 minutes in anti-mouse IgG electrochemiluminescence (ECL) HRP-linked secondary antibody (diluted in 2.5% milk/TBS-T at 1:10,000; Amersham Biosciences, UK), then rinsed for 30 minutes in TBS-T, all shaking at room temperature. To visualize the HRP-conjugated secondary antibodies, the membranes were incubated in Pierce ECL Western Blotting Substrate (Thermo Scientific, Waltham, MA) for 10 minutes, exposed to Kodak BioMax MS film (Kodak, Rochester, NY) for 30 seconds to 5 minutes, and developed in a Kodak processor.

2.8. Autoradiographic ('radiospotblot') analysis of PiB binding

For quantitative analysis of high-affinity PiB binding sites, temporal cortical homogenates (20% w/v) were centrifuged at 3,000 *×g* for five minutes and 2.5μl of the clarified supernatant pipetted in duplicate onto silanized Superfrost Plus microscope slides (Fisher Thermo Scientific, Waltham, MA), dried on a slide warmer at 37°C overnight, and stored in an airtight container at −80°C until use. The slides were brought to room temperature in air-tight containers and then immersion-fixed in 10% ethanol/PBS for 20 minutes. They were incubated with 1.0nM ^{3}H-PiB (SA=82 Ci/mmol, custom synthesis, GE Healthcare, UK) (Rosen, et al., 2011) in 5% ethanol/PBS for one hour at room temperature, rinsed 2 times with 10% ethanol/PBS and 2 times with deionized H_2O, both on ice, and then air-dried before direct apposition to ^{3}H-Hyperfilm (GE Amersham, UK). After a 4-week exposure, the film was developed with D19 developing solution (Kodak, New Haven, CT), and images were captured with a QICAM digital camera (QImaging, Surrey, BC, Canada). The intensity of ^{3}H-induced darkening was quantified for each sample blot using Photoshop.

2.9. Seeding Aβ deposition in transgenic mice with primate brain extracts

To assess the ability of Aβ-laden brain extracts from squirrel monkeys to seed cerebral Aβ deposition in transgenic mice, eight 13-15-week old female APP/PS1 mice were anesthetized with isoflurane gas and readied for sterile stereotaxic surgery. 10% clarified cortical extract was prepared from two AD cases and two aged squirrel monkeys (two mice were injected with extract from each donor; see Table 1). 2.5μl of extract was injected unilaterally into the dorsal hippocampus at a rate of 0.5μl/min at the following coordinates: −2.2 A/P; +/−1.8 ML; −1.9 DV (Franklin and Paxinos, 2007). As an internal control, sterile PBS (2.5μl) was injected into the contralateral hippocampus. Post-operatively, the mice were treated with 0.05 mg/kg buprenorphine to minimize discomfort from the surgery. 22 weeks following surgery, the mice were euthanized by an overdose of isoflurane and transcardially perfused with de-polymerized 4% paraformaldehyde (4-8°C) in phosphate buffer.

2.10. Statistical analyses

Analysis of variance (ANOVA) or *t*-tests (both two-tailed tests) were used to assess group differences. For the radiospotblot results, an unpaired *t*-test was used to assess differences in the PiB-binding signal between AD and nonhuman primate tissue homogenates.

3. Results

3.1. Squirrel monkeys develop extensive cerebral β-amyloidosis in old age

Within the context of normal inter-individual variation (Heuer, et al., 2012,Walker and Cork, 1999), Aβ immunohistochemistry revealed species-typical patterns of Aβ deposition. A consistent characteristic of aged squirrel monkeys (and of nonhuman primates in general) is a relative abundance of cerebral amyloid-β angiopathy (CAA), particularly in capillaries (Heuer, et al., 2012), and this was the case in the 7 squirrel monkeys analyzed in this study. In contrast, CAA was relatively sparse in the 9 AD cases examined, and was mostly confined to larger vessels. In both species, at least some Aβ-immunoreactive lesions were detected by all antibodies to Aβ that we employed, including N-terminal antibodies 6E10 and 8E1 (Figure 1), mid-sequence antibody 4G8, and C-terminal antibodies R361 and R398 (not shown).

By ELISA, the mean levels of insoluble Aβ40 and Aβ42 in monkeys sometimes equaled or exceeded the levels in AD samples (Table 1). Regarding the relative amounts of the two isoforms in individuals, insoluble Aβ42 was more abundant than Aβ40 in both cortical regions of all humans and in 4 of the 6 squirrel monkeys analyzed. Aβ40 was the most abundant peptide in the temporal cortex of both Ss1 and Ss2, and in the occipital cortex of Ss2 only (Table 1).

The presence of abundant Aβ was confirmed by immunoblot analysis of samples from AD cases and aged squirrel monkeys, two of which had very high levels of Aβ (Figure 2). As expected, SDS-stable dimers and trimers were present in extracts from the AD brain, but also in brain extracts from older squirrel monkeys. Compared to the AD brain extracts, trimers from the squirrel monkey brain exhibited greater immunoreactivity to an N-terminal Aβ antibody (6E10), and less immunoreactivity to a mid-sequence antibody (4G8) (Figure 2). With regard to APP, antibody 6E10 revealed a more strongly immunostained band in squirrel monkeys, whereas 4G8 detected a stronger band in AD cases.

3.2. Tauopathy is rare in aged squirrel monkeys

Rare cells and neurites were immunoreactive with antibodies to hyperphosphorylated tau in aged squirrel monkeys, but these were very sparse, and unlike in AD, the hippocampus was largely devoid of tauopathy (Figure 3).

3.3. Aβ peptide populations are similar in aged squirrel monkeys and humans with AD

To identify full-length and modified Aβ sequences, total Aβ peptide populations immunoprecipitated from temporal and occipital neocortical tissue samples were analyzed in a MALDI-TOF mass spectrometer to measure the mass and charge of each peptide. Although there was variation in the pattern of fragments among individual subjects and between the two brain areas, the overall analysis of both buffer-soluble and formic acid-solubilized, buffer-insoluble fractions indicated that all of the major Aβ fragments that are present in the AD brain also occur in aged squirrel monkeys, including Aβ1-40, Aβ1-42, Aβ1-34, Aβ4-40, Aβ4-42, AβpE3-40, AβpE3-42, and oxidized forms of Aβ1-40 and Aβ1-42. Figure 4 illustrates the general similarity of insoluble Aβ fragments in two aged squirrel

monkeys (Panel A) and two AD cases (Panel B) whereas the table (Panel C) lists the values of the acquired experimental masses for all of the identified formic acid-soluble Aβ fragments in the specimens tested. As expected, very few (if any) Aβ fragments were detected in the non-demented humans (not shown).

3.4. Specific high-affinity binding of PiB is low in squirrel monkey cortical extracts

In light of the general similarity of Aβ isoforms and tissue deposits in humans and nonhuman primates, we sought to substantiate our previous finding that human Aβ displays relatively more abundant high-affinity PiB-binding sites per molecule of Aβ (Rosen, et al., 2011). To this end, we used a “radiospotblot” assay in which cortical extracts are dried onto glass slides and then ^{3}H-PiB binding is analyzed by standard autoradiography. Compared to the previous filtration assay (Rosen, et al., 2011), in which very small multimers might be lost to detection, the radiospotblot technique has the advantage of including all multimeric Aβ in the assayed sample. Quantitative analysis confirmed that extracts from AD temporal cortex contain significantly more high-affinity PiB binding sites per molecule of Aβ than do comparable extracts from aged squirrel monkeys with a heavy burden of Aβ (Figure 5).

3.5. Cortical extracts from aged squirrel monkeys seed Aβ deposition in APP/PS1 transgenic mice

To determine whether Aβ-rich cortical extracts from nonhuman primates, like extracts from AD patients (Kane, et al., 2000) and aged APP-transgenic mice (Meyer-Luehmann, et al., 2006), are able to seed the deposition of Aβ, temporal cortical extracts from 2 AD cases and 2 squirrel monkeys were injected into the dorsal hippocampus of APP/PS1 transgenic mice. Aβ immunohistochemistry revealed similar induction and re-distribution of Aβ deposition by AD and squirrel monkey brain extracts (Figure 6).

4. Discussion

Despite ample Aβ deposition in the senescent brain, no nonhuman primate has yet been found to develop the full phenotype of Alzheimer's disease, including widespread neurofibrillary tangles, loss of cortical and hippocampal neurons, brain atrophy, and dementia (Finch and Austad, 2015,Heuer, et al., 2012,Walker and Cork, 1999). Given the importance of Aβ aggregation in the ontogeny of AD (Hardy and Selkoe, 2002,Holtzman, et al., 2011), nonhuman primates present an exceptional opportunity to reveal the molecular properties of Aβ that drive the disease process in humans. Monkeys manifest a relatively uncomplicated form of non-AD brain aging, unlike high-pathology but cognitively normal humans, who may simply be at an early stage of AD pathogenesis (Jack, et al., 2010). Our findings show that, despite species-typical phenotypic differences in the nature of Aβ deposition (Heuer, et al., 2012), the array of Aβ variants and the ability of misfolded Aβ to induce aggregation *in vivo* are highly similar in brain tissues from humans with AD and aged squirrel monkeys. However, a distinctly high affinity of PiB for human Aβ and differences in epitope affinity on semi-denaturing gels signify the possible existence of strain-like architectural and/or compositional differences in Aβ molecules and cofractionating components among species.

In AD, the accumulated Aβ peptide varies at both its N- and C-termini, and these variations influence the peptide's disease-relevant properties - tendency to aggregate, toxicity, and solubility (Jonson, et al., 2015,Piccini, et al., 2005,Pike, et al., 1995). Aβ40 is the main isoform generated by brain cells, but Aβ42 has two additional hydrophobic residues at the C-terminal end that augment aggregation; consequently, Aβ42 is thought to be especially important in the early development of AD (Holtzman, et al., 2011). Truncated and modified Aβ isoforms are detected in human brain and cerebrospinal fluid (Miravalle, et al., 2005,Portelius, et al., 2010a,Portelius, et al., 2010b,Portelius, et al., 2015,Portelius, et al., 2006,Rufenacht, et al., 2005,Struyfs, et al., 2015,Tekirian, et al., 1996,Tekirian, et al., 1998), and the relative amounts of full-length and modified Aβ isoforms may play a role in the peptide's pathogenicity. Portelius and colleagues used MALDI-TOF MS to demonstrate that patients with AD tend to have more N-terminally truncated and pyroglutamated forms and less Aβ1-40 than do nondemented human subjects with extensive Aβ levels (Portelius, et al., 2015). Using western blotting, Piccini and colleagues identified an AD-specific population of soluble Aβ1-42, Aβ[pE3]-42, and Aβ[pE11]-42 peptides in frontal cortical extracts, and showed that synthetic “AD-like” preparations of these 3 Aβ isoforms had enhanced cytotoxicity when compared to synthetic Aβ peptides prepared in ratios detected in nondemented humans (Piccini, et al., 2005). N-terminally truncated Aβ isoforms bearing pyroglutamate (Aβ[pE3]-x and Aβ[pE11]-x) have a stronger tendency to aggregate than do Aβ1-40 and Aβ1-42; they also are more resistant to proteolysis, and are less soluble as a result of their greater hydrophobicity (Kuo, et al., 1997,Miravalle, et al., 2005,Roher, et al., 1993,Schlenzig, et al., 2009,Tekirian, et al., 1999). In addition to its manifest cytotoxicity (Alexandru, et al., 2011,Becker, et al., 2013,Gillman, et al., 2014,Jonson, et al., 2015,Nussbaum, et al., 2012,Schlenzig, et al., 2012), the amount of pyroglutamate Aβ has been reported to correlate with cognitive decline in humans (Morawski, et al., 2014). Although we detected Aβ-truncated species bearing pyroglutamate at position 3 in both human and squirrel monkey specimens, as illustrated in Figure 4, derivatives with the same post-translational modification but starting at position 11 were not clearly evident in our sample set of human and simian cases. These differences may relate to the particular specimens analyzed in our experimental paradigm; alternatively, their absence in both sample sets could reflect low peptide recovery during the tissue extraction procedure due to the enhanced aggregation properties of pyroglutamate species, resulting in peptide concentrations falling below the MS detection levels.

Our MALDI TOF MS analysis of cortical samples did not clearly identify an Aβ peptide or group of Aβ isoforms that occurred exclusively in AD subjects or in senescent squirrel monkeys. In a preliminary analysis of occipital cortical samples, we have also found that the Aβ peptide profile of aged rhesus monkeys (*Macaca mulatta*) is similar to that in humans and squirrel monkeys (R.F. Rosen et al., unpublished). The presence of similarly cleaved Aβ fragments in the aged nonhuman primate brain suggests that functionally similar peptidases proteolyze Aβ aggregates in humans and nonhuman primates, and that the pathogenicity of multimeric Aβ in AD cannot be unambiguously attributed to the presence or absence of a specific Aβ fragment. Overall, these findings indicate that, in humans and nonhuman primates, Aβ is subject to similarly diverse cleavage events and post-translational modifications.

Whereas the presence of specific Aβ types appears not to explain the pathogenicity of the peptide in humans, the relative amounts of different Aβ isoforms may be important. The ratio of Aβ42:Aβ40 influences the aggregation and toxicity of the peptide (Chang and Chen, 2014,Jan, et al., 2008,Kuperstein, et al., 2010,Murray, et al., 2009,Pauwels, et al., 2012). In mouse models, Aβ40 is less amyloidogenic than is Aβ42 (McGowan, et al., 2005), and when present at sufficient levels, Aβ40 may actually inhibit the deposition of Aβ in brain (Kim, et al., 2007). Older nondemented humans with high Aβ load ('pathological aging') tend to have relatively higher amounts of Aβ1-40 than do AD patients (Portelius, et al., 2015). In humans, approximately 90% of secreted Aβ is Aβ40 (Selkoe, 1999), but in AD, more senile plaques are immunohistochemically positive for Aβ42 than Aβ40 (Walker, et al., 2000). In contrast, Aβ40 was found to be the predominant peptide isoform in nonhuman primate Aβ lesions by immunohistochemistry (Elfenbein, et al., 2007,Gearing, et al., 1996). However, biochemical analysis of Aβ in an aged squirrel monkey brain revealed levels of insoluble Aβ42 much higher than would have been predicted based on immunohistochemical findings (Sawamura, et al., 1997). Our ELISA analyses confirm that the mean ratio of insoluble Aβ42:Aβ40 tends to be lower in nonhuman primates than in humans, but this ratio varies among animals, and in some monkeys it is comparable to that in humans with AD (Table 1). It may be informative that the animals with the most total Aβ also had the lowest Aβ42:Aβ40 ratio; this could indicate: a) that Aβ40 accumulates preferentially after the initial aggregation of Aβ42; b) that Aβ42 in the lesions has been trimmed to Aβ40 by exopeptidases; and/or c) that the deposition of Aβ40 and Aβ42 proceeds by different means in different animals. The discovery of an unusual case of AD with very high levels of Aβ and a preponderance of Aβ40 (Rosen, et al., 2010a) suggests that similar mechanisms are possible in humans.

Species-typical patterns of cerebral Aβ deposition may result from distinct Aβ aggregation pathways or variations in the multidimensional structure of pathogenic Aβ (i.e., Aβ 'strains') (Levine and Walker, 2010,Rosen, et al., 2011). Using western blotting (Rosen, et al., 2010b), we identified SDS-stable dimers and trimers in extracts from the AD brain, as expected, but we also detected these dimers and trimers in extracts from several older squirrel monkeys (Figure 2). Trimers from the monkey brain exhibited enhanced immunoreactivity to an N-terminal Aβ antibody (6E10), as compared to AD brain-derived trimers. Conversely, the 4G8 antibody to Aβ17-24 showed greater binding to trimers from the AD brain compared to the monkey brain. These findings suggest that multimeric Aβ species in humans and nonhuman primates have distinct epitope availabilities and therefore may not share an identical tertiary/quaternary structure, which in turn could influence their pathogenicity (Cohen, et al., 2015). Additional studies are needed to confirm these findings and to establish whether the oligomeric bands on semi-denaturing gels represent bona fide, pre-existing oligomers, or are an artifact of the preparation and analysis of the extracts (Bitan, et al., 2005,Bitan, et al., 2003,Hepler, et al., 2006,Watt, et al., 2013). Even if the bands do not represent oligomers that existed in the living brain, differences in their quantity and immunoreactivity could furnish useful clues to the nature and variability of multimeric Aβ. A recent study reported that an incipient tauopathy can be induced in cynomolgus monkeys (*Macaca fascicularis*) by the intraventricular injection of synthetic Aβ oligomers (Forny-Germano, et al., 2014). While the physical characteristics of bioactive oligomers *in vivo* are not yet fully understood, it

may be informative to establish the relative pathogenic potency of Aβ oligomers originating the AD patients and aged monkeys.

Our previous PiB radioligand binding analysis of tissue samples found that – unlike in AD – high-affinity PiB binding sites are negligible in Aβ aggregates from the brains of aged nonhuman primates (Rosen, et al., 2011). Others have shown that high-affinity PiB binding sites are also sparse on synthetic Aβ fibrils and aggregated Aβ from the brains of APP transgenic mice (Klunk, et al., 2005,Maeda, et al., 2007,Serdons, et al., 2009,Toyama, et al., 2005). In the present study, we extended our previous findings using a "radiospotblot" technique that enables the quantification of PiB binding in human and simian cortical extracts without a liquid scintillation counter, while maintaining a satisfactory signal-to-noise ratio. Additionally, because the extract is dried onto a charged glass slide before incubation with ^{3}H-PiB, there is no need for membrane filtration, and less chance that very small Aβ assemblies are lost to detection. The radiospotblot experiment confirmed the relative paucity of high-affinity PiB binding sites associated with aggregated simian Aβ, supporting the possibility that Aβ folds into structurally distinct strains in AD compared to aged monkeys. The generation of variant strains may, in turn, be influenced by the presence of co-factors that differentially modulate the aggregation of Aβ (Wilhelmus, et al., 2007) or its ability to bind PiB, but to date no such molecules have been identified.

Evidence for Aβ strains raises the further question of whether such variants can occur intraspecifically, particularly in humans. Differences in the molecular ratio of bound PiB to Aβ among human AD cases have been reported (Ikonomovic, et al., 2012,Rosen, et al., 2010a,Scholl, et al., 2012). Furthermore, in two clinically different cases of AD, solid-state nuclear magnetic resonance analysis of derived fibers revealed evidence for Aβ aggregates with differing fibrillar ultrastructure and molecular architecture (Lu, et al., 2013). Such proteopathic strains could help to explain both the complex pathobiology of Aβ and the paradoxical absence of dementia in some humans with a heavy burden of senile plaques.

Aβ-rich brain extracts from aged monkeys induce Aβ deposition in the brains of APP/PS1-transgenic mice in a prion-like manner (Figure 6), similar to seeding by brain extracts from AD and APP-transgenic mouse donors (Eisele, et al., 2009,Eisele, et al., 2010,Fritschi, et al., 2014,Hamaguchi, et al., 2012,Heilbronner, et al., 2013,Kane, et al., 2000,Langer, et al., 2011,Meyer-Luehmann, et al., 2006,Morales, et al., 2015,Morales, et al., 2012,Rosen, et al., 2012,Stohr, et al., 2014,Stohr, et al., 2012,Walker, et al., 2002,Watts, et al., 2014,Watts, et al., 2011,Ye, et al., 2015a,Ye, et al., 2015b). Aggregated synthetic Aβ peptides, though able to seed Aβ deposition *in vivo* (Stohr, et al., 2014,Stohr, et al., 2012), are much less potent than are Aβ seeds generated within the brain (Stohr, et al., 2012). As shown in our radiospotblot experiment (above), Aβ fibrils from aged monkeys, like synthetic Aβ, have relatively few high-affinity PiB-binding sites. The deposits in host mice seeded by AD brain extracts and squirrel monkey brain extracts stained similarly for both Aβ40 and Aβ42, despite the fact that the squirrel monkey brain extracts had lower Aβ42:Aβ40 ratios than did the AD brain extracts. Thus, the extent to which the seeded deposits recapitulate the strain-like features of Aβ in the host, the donor, or both (Meyer-Luehmann, et al., 2006) remains to be established.

It is possible that, given a longer lifespan, some senescent nonhuman primates would eventually manifest AD. The emergence of Aβ plaques and neurofibrillary tangles in the human brain precedes the onset of clinical dementia by at least 10-20 years (Bateman, et al., 2012,Buchhave, et al., 2012,Holtzman, et al., 2011,Jack and Holtzman, 2013,Sperling, et al., 2013). The longer lifespan of humans (Finch and Sapolsky, 1999) could permit changes in Aβ such as post-translational modifications that influence its pathobiology (Lowenson, et al., 1999). However, we found that the amount of Aβ in some aged squirrel monkeys exceeded the mean levels in humans with AD (Table 1), but in the absence of AD-like tauopathy. In light of generally similar populations of Aβ fragments, the divergent degree of PiB binding and epitope exposure implicates the multidimensional configuration of Aβ as an important element in the pathogenic cascade leading to tauopathy and AD in humans. The molecular architecture of Aβ assemblies may, in turn, be influenced by the relative involvement of different Aβ fragments/isoforms or molecular chaperones in their construction. While neither the overall quantity of Aβ nor a high Aβ42:Aβ40 ratio appears to be sufficient to impel an AD-like neurodegenerative cascade in nonhuman primates, the Aβ42:Aβ40 ratio and other post-translational influences are worth further study, as these could disclose new means of reducing the pathogenicity of Aβ in AD.

5. Conclusions

Aged nonhuman primates manifest extensive cerebral deposition of Aβ, yet only humans develop all of the clinicopathologic characteristics of AD. Our findings show that the isoform populations of cerebral Aβ in humans and aged squirrel monkeys are remarkably similar, and that Aβ-laden brain extracts from monkeys and humans similarly induce the accumulation of Aβ deposition in APP/PS1-transgenic mice. On the other hand, aggregated Aβ in aged squirrel monkeys displays distinctive epitope exposure in immunoblots and is deficient in high-affinity binding sites for PiB. These data reinforce the hypothesis that the pathogenicity of Aβ aggregates is modulated by molecular conformational variations in the protein. Comparison of naturally occurring Aβ multimers in nonhuman primates with those in the human AD brain may help to disclose the mechanisms that underlie the distinctively human vulnerability to AD.

Acknowledgments

We gratefully acknowledge the donation of tissues and/or helpful conversations with A. Arnsten (Yale), M.L. Voytko (Wake Forest), D. Lyons (Stanford), M. Gearing (Emory), M.P. Murphy (Kentucky), J. Lah (Emory), H.-U. Demuth (Fraunhofer Institute for Cell Therapy & Immunology) and D.L. Rosene (Boston University). This work was supported by P51RR165, P51OD11132, R21NS077049, P30 NS050276, P50AG025688, and the MetLife Foundation. Additional support was provided by P01AG026423, R21NS080576, R21AG051266 and the BrightFocus Foundation.

References

Alexandru A, Jagla W, Graubner S, Becker A, Bauscher C, Kohlmann S, Sedlmeier R, Raber KA, Cynis H, Ronicke R, Reymann KG, Petrasch-Parwez E, Hartlage-Rubsamen M, Waniek A, Rossner S, Schilling S, Osmand AP, Demuth HU, von Horsten S. Selective hippocampal neurodegeneration in transgenic mice expressing small amounts of truncated Abeta is induced by pyroglutamate-Abeta formation. J Neurosci. 2011; 31(36):12790–801. doi:10.1523/JNEUROSCI.1794-11.2011. [PubMed: 21900558]

Arriagada PV, Marzloff K, Hyman BT. Distribution of Alzheimer-type pathologic changes in nondemented elderly individuals matches the pattern in Alzheimer's disease. Neurology. 1992; 42(9):1681–8. [PubMed: 1307688]

Bakota L, Brandt R. Tau Biology and Tau-Directed Therapies for Alzheimer's Disease. Drugs. 2016; 76(3):301–13. doi:10.1007/s40265-015-0529-0. [PubMed: 26729186]

Bateman RJ, Xiong C, Benzinger TL, Fagan AM, Goate A, Fox NC, Marcus DS, Cairns NJ, Xie X, Blazey TM, Holtzman DM, Santacruz A, Buckles V, Oliver A, Moulder K, Aisen PS, Ghetti B, Klunk WE, McDade E, Martins RN, Masters CL, Mayeux R, Ringman JM, Rossor MN, Schofield PR, Sperling RA, Salloway S, Morris JC, Dominantly Inherited Alzheimer N. Clinical and biomarker changes in dominantly inherited Alzheimer's disease. N Engl J Med. 2012; 367(9):795–804. doi:10.1056/NEJMoa1202753. [PubMed: 22784036]

Becker A, Kohlmann S, Alexandru A, Jagla W, Canneva F, Bauscher C, Cynis H, Sedlmeier R, Graubner S, Schilling S, Demuth HU, von Horsten S. Glutaminyl cyclase-mediated toxicity of pyroglutamate-beta amyloid induces striatal neurodegeneration. BMC Neurosci. 2013; 14:108. doi: 10.1186/1471-2202-14-108. [PubMed: 24083638]

Bierer LM, Hof PR, Purohit DP, Carlin L, Schmeidler J, Davis KL, Perl DP. Neocortical neurofibrillary tangles correlate with dementia severity in Alzheimer's disease. Arch Neurol. 1995; 52(1):81–8. [PubMed: 7826280]

Bilousova T, Miller CA, Poon WW, Vinters HV, Corrada M, Kawas C, Hayden EY, Teplow DB, Glabe C, Albay R 3rd, Cole GM, Teng E, Gylys KH. Synaptic Amyloid-beta Oligomers Precede p-Tau and Differentiate High Pathology Control Cases. Am J Pathol. 2016; 186(1):185–98. doi:10.1016/j.ajpath.2015.09.018. [PubMed: 26718979]

Bitan G, Fradinger EA, Spring SM, Teplow DB. Neurotoxic protein oligomers--what you see is not always what you get. Amyloid. 2005; 12(2):88–95. doi:10.1080/13506120500106958. [PubMed: 16011984]

Bitan G, Kirkitadze MD, Lomakin A, Vollers SS, Benedek GB, Teplow DB. Amyloid beta -protein (Abeta) assembly: Abeta 40 and Abeta 42 oligomerize through distinct pathways. Proc Natl Acad Sci U S A. 2003; 100(1):330–5. doi:10.1073/pnas.222681699. [PubMed: 12506200]

Borchelt DR, Ratovitski T, van Lare J, Lee MK, Gonzales V, Jenkins NA, Copeland NG, Price DL, Sisodia SS. Accelerated amyloid deposition in the brains of transgenic mice coexpressing mutant presenilin 1 and amyloid precursor proteins. Neuron. 1997; 19(4):939–45. [PubMed: 9354339]

Buchhave P, Minthon L, Zetterberg H, Wallin AK, Blennow K, Hansson O. Cerebrospinal fluid levels of beta-amyloid 1-42, but not of tau, are fully changed already 5 to 10 years before the onset of Alzheimer dementia. Arch Gen Psychiatry. 2012; 69(1):98–106. doi:10.1001/archgenpsychiatry.2011.155. [PubMed: 22213792]

Catalano SM, Dodson EC, Henze DA, Joyce JG, Krafft GA, Kinney GG. The role of amyloid-beta derived diffusible ligands (ADDLs) in Alzheimer's disease. Curr Top Med Chem. 2006; 6(6):597–608. [PubMed: 16712494]

Chang YJ, Chen YR. The coexistence of an equal amount of Alzheimer's amyloid-beta 40 and 42 forms structurally stable and toxic oligomers through a distinct pathway. FEBS J. 2014; 281(11):2674–87. doi:10.1111/febs.12813. [PubMed: 24720730]

Chen X, Errangi B, Li L, Glasser MF, Westlye LT, Fjell AM, Walhovd KB, Hu X, Herndon JG, Preuss TM, Rilling JK. Brain aging in humans, chimpanzees (Pan troglodytes), and rhesus macaques (Macaca mulatta): magnetic resonance imaging studies of macro-and microstructural changes. Neurobiol Aging. 2013; 34(10):2248–60. doi:10.1016/j.neurobiolaging.2013.03.028. [PubMed: 23623601]

Cohen ML, Kim C, Haldiman T, ElHag M, Mehndiratta P, Pichet T, Lissemore F, Shea M, Cohen Y, Chen W, Blevins J, Appleby BS, Surewicz K, Surewicz WK, Sajatovic M, Tatsuoka C, Zhang S, Mayo P, Butkiewicz M, Haines JL, Lerner AJ, Safar JG. Rapidly progressive Alzheimer's disease features distinct structures of amyloid-beta. Brain. 2015; 138(Pt 4):1009–22. doi:10.1093/brain/awv006. [PubMed: 25688081]

Crystal H, Dickson D, Fuld P, Masur D, Scott R, Mehler M, Masdeu J, Kawas C, Aronson M, Wolfson L. Clinico-pathologic studies in dementia: nondemented subjects with pathologically confirmed Alzheimer's disease. Neurology. 1988; 38(11):1682–7. [PubMed: 3185902]

D'Angelo OM, Dooyema J, Courtney C, Walker LC, Heuer E. Cerebral amyloid angiopathy in an aged sooty mangabey (Cercocebus atys). Comp Med. 2013; 63(6):515–20. [PubMed: 24326228]

Eisele YS, Bolmont T, Heikenwalder M, Langer F, Jacobson LH, Yan ZX, Roth K, Aguzzi A, Staufenbiel M, Walker LC, Jucker M. Induction of cerebral beta-amyloidosis: intracerebral versus systemic Abeta inoculation. Proc Natl Acad Sci U S A. 2009; 106(31):12926–31. doi:10.1073/pnas.0903200106. [PubMed: 19622727]

Eisele YS, Obermuller U, Heilbronner G, Baumann F, Kaeser SA, Wolburg H, Walker LC, Staufenbiel M, Heikenwalder M, Jucker M. Peripherally applied Abeta-containing inoculates induce cerebral beta-amyloidosis. Science. 2010; 330(6006):980–2. doi:10.1126/science.1194516. [PubMed: 20966215]

Elfenbein HA, Rosen RF, Stephens SL, Switzer RC, Smith Y, Pare J, Mehta PD, Warzok R, Walker LC. Cerebral beta-amyloid angiopathy in aged squirrel monkeys. Histol Histopathol. 2007; 22(2):155–67. [PubMed: 17149688]

Fast R, Rodell A, Gjedde A, Mouridsen K, Alstrup AK, Bjarkam CR, West MJ, Berendt M, Moller A. PiB Fails to Map Amyloid Deposits in Cerebral Cortex of Aged Dogs with Canine Cognitive Dysfunction. Front Aging Neurosci. 2013; 5:99. doi:10.3389/fnagi.2013.00099. [PubMed: 24416017]

Ferreira ST, Lourenco MV, Oliveira MM, De Felice FG. Soluble amyloid-beta oligomers as synaptotoxins leading to cognitive impairment in Alzheimer's disease. Front Cell Neurosci. 2015; 9:191. doi:10.3389/fncel.2015.00191. [PubMed: 26074767]

Finch CE, Austad SN. Primate aging in the mammalian scheme: the puzzle of extreme variation in brain aging. Age (Dordr). 2012; 34(5):1075–91. doi:10.1007/s11357-011-9355-9. [PubMed: 22218781]

Finch CE, Austad SN. Commentary: is Alzheimer's disease uniquely human? Neurobiol Aging. 2015; 36(2):553–5. doi:10.1016/j.neurobiolaging.2014.10.025. [PubMed: 25533426]

Finch CE, Sapolsky RM. The evolution of Alzheimer disease, the reproductive schedule, and apoE isoforms. Neurobiol Aging. 1999; 20(4):407–28. [PubMed: 10604433]

Forny-Germano L, Lyra e Silva NM, Batista AF, Brito-Moreira J, Gralle M, Boehnke SE, Coe BC, Lablans A, Marques SA, Martinez AM, Klein WL, Houzel JC, Ferreira ST, Munoz DP, De Felice FG. Alzheimer's disease-like pathology induced by amyloid-beta oligomers in nonhuman primates. J Neurosci. 2014; 34(41):13629–43. doi:10.1523/JNEUROSCI.1353-14.2014. [PubMed: 25297091]

Franklin, KBJ.; Paxinos, G. The mouse brain in stereotaxic coordinates. 3rd ed.. Oxford; Elsevier, Amsterdam: 2007.

Fritschi SK, Cintron A, Ye L, Mahler J, Buhler A, Baumann F, Neumann M, Nilsson KP, Hammarstrom P, Walker LC, Jucker M. Abeta seeds resist inactivation by formaldehyde. Acta Neuropathol. 2014; 128(4):477–84. doi:10.1007/s00401-014-1339-2. [PubMed: 25193240]

Gearing M, Tigges J, Mori H, Mirra SS. A beta40 is a major form of beta-amyloid in nonhuman primates. Neurobiol Aging. 1996; 17(6):903–8. doi:S0197458096001649 [pii]. [PubMed: 9363802]

Gearing M, Tigges J, Mori H, Mirra SS. beta-Amyloid (A beta) deposition in the brains of aged orangutans. Neurobiol Aging. 1997; 18(2):139–46. [PubMed: 9258890]

Geula C, Nagykery N, Wu CK. Amyloid-beta deposits in the cerebral cortex of the aged common marmoset (Callithrix jacchus): incidence and chemical composition. Acta Neuropathol (Berl). 2002; 103(1):48–58. [PubMed: 11837747]

Gillman AL, Jang H, Lee J, Ramachandran S, Kagan BL, Nussinov R, Teran Arce F. Activity and architecture of pyroglutamate-modified amyloid-beta (AbetapE3- 42) pores. The journal of physical chemistry B. 2014; 118(26):7335–44. doi:10.1021/jp5040954. [PubMed: 24922585]

Hamaguchi T, Eisele YS, Varvel NH, Lamb BT, Walker LC, Jucker M. The presence of Abeta seeds, and not age per se, is critical to the initiation of Abeta deposition in the brain. Acta Neuropathol. 2012; 123(1):31–7. doi:10.1007/s00401-011-0912-1. [PubMed: 22101366]

Hamley IW. The amyloid beta peptide: a chemist's perspective. Role in Alzheimer's and fibrillization. Chem Rev. 2012; 112(10):5147–92. doi:10.1021/cr3000994. [PubMed: 22813427]

Hardy J, Selkoe DJ. The amyloid hypothesis of Alzheimer's disease: progress and problems on the road to therapeutics. Science. 2002; 297(5580):353–6. doi:10.1126/science.1072994 297/5580/353 [pii]. [PubMed: 12130773]

Hatami A, Albay R 3rd, Monjazeb S, Milton S, Glabe C. Monoclonal antibodies against Abeta42 fibrils distinguish multiple aggregation state polymorphisms in vitro and in Alzheimer disease brain. J Biol Chem. 2014; 289(46):32131–43. doi:10.1074/jbc.M114.594846. [PubMed: 25281743]

Head E. A canine model of human aging and Alzheimer's disease. Biochim Biophys Acta. 2013; 1832(9):1384–9. doi:10.1016/j.bbadis.2013.03.016. [PubMed: 23528711]

Heilbronner G, Eisele YS, Langer F, Kaeser SA, Novotny R, Nagarathinam A, Aslund A, Hammarstrom P, Nilsson KP, Jucker M. Seeded strain-like transmission of beta-amyloid morphotypes in APP transgenic mice. EMBO reports. 2013; 14(11):1017–22. doi:10.1038/embor.2013.137. [PubMed: 23999102]

Hepler RW, Grimm KM, Nahas DD, Breese R, Dodson EC, Acton P, Keller PM, Yeager M, Wang H, Shughrue P, Kinney G, Joyce JG. Solution state characterization of amyloid beta-derived diffusible ligands. Biochemistry. 2006; 45(51):15157–67. doi:10.1021/bi061850f. [PubMed: 17176037]

Herndon JG, Tigges J, Anderson DC, Klumpp SA, McClure HM. Brain weight throughout the life span of the chimpanzee. J Comp Neurol. 1999; 409(4):567–72. [PubMed: 10376740]

Herndon JG, Tigges J, Klumpp SA, Anderson DC. Brain weight does not decrease with age in adult rhesus monkeys. Neurobiol Aging. 1998; 19(3):267–72. [PubMed: 9662002]

Heuer E, Rosen RF, Cintron A, Walker LC. Nonhuman primate models of Alzheimer-like cerebral proteopathy. Current pharmaceutical design. 2012; 18(8):1159–69. [PubMed: 22288403]

Holtzman DM, Morris JC, Goate AM. Alzheimer's disease: the challenge of the second century. Science translational medicine. 2011; 3(77):77sr1. doi:10.1126/scitranslmed.3002369. [PubMed: 21471435]

Ikonomovic MD, Abrahamson EE, Price JC, Hamilton RL, Mathis CA, Paljug WR, Debnath ML, Cohen AD, Mizukami K, DeKosky ST, Lopez OL, Klunk WE. Early AD pathology in a [C-11]PiB-negative case: a PiB-amyloid imaging, biochemical, and immunohistochemical study. Acta Neuropathol. 2012; 123(3):433–47. doi:10.1007/s00401-012-0943-2. [PubMed: 22271153]

Jack CR Jr. Holtzman DM. Biomarker modeling of Alzheimer's disease. Neuron. 2013; 80(6):1347–58. doi:10.1016/j.neuron.2013.12.003. [PubMed: 24360540]

Jack CR Jr. Knopman DS, Jagust WJ, Shaw LM, Aisen PS, Weiner MW, Petersen RC, Trojanowski JQ. Hypothetical model of dynamic biomarkers of the Alzheimer's pathological cascade. Lancet Neurol. 2010; 9(1):119–28. doi:10.1016/S1474-4422(09)70299-6. [PubMed: 20083042]

Jan A, Gokce O, Luthi-Carter R, Lashuel HA. The ratio of monomeric to aggregated forms of Abeta40 and Abeta42 is an important determinant of amyloid-beta aggregation, fibrillogenesis, and toxicity. J Biol Chem. 2008; 283(42):28176–89. doi:10.1074/jbc.M803159200. [PubMed: 18694930]

Jonson M, Pokrzywa M, Starkenberg A, Hammarstrom P, Thor S. Systematic Abeta Analysis in Drosophila Reveals High Toxicity for the 1-42, 3-42 and 11-42 Peptides, and Emphasizes N-and C-Terminal Residues. PLoS One. 2015; 10(7):e0133272. doi:10.1371/journal.pone.0133272. [PubMed: 26208119]

Jucker M. The benefits and limitations of animal models for translational research in neurodegenerative diseases. Nat Med. 2010; 16(11):1210–4. doi:10.1038/nm.2224. [PubMed: 21052075]

Kane MD, Lipinski WJ, Callahan MJ, Bian F, Durham RA, Schwarz RD, Roher AE, Walker LC. Evidence for seeding of beta -amyloid by intracerebral infusion of Alzheimer brain extracts in beta -amyloid precursor protein-transgenic mice. J Neurosci. 2000; 20(10):3606–11. [PubMed: 10804202]

Kim J, Onstead L, Randle S, Price R, Smithson L, Zwizinski C, Dickson DW, Golde T, McGowan E. Abeta40 inhibits amyloid deposition in vivo. J Neurosci. 2007; 27(3):627–33. [PubMed: 17234594]

Klunk WE, Lopresti BJ, Ikonomovic MD, Lefterov IM, Koldamova RP, Abrahamson EE, Debnath ML, Holt DP, Huang GF, Shao L, DeKosky ST, Price JC, Mathis CA. Binding of the positron emission tomography tracer Pittsburgh compound-B reflects the amount of amyloid-beta in

Alzheimer's disease brain but not in transgenic mouse brain. J Neurosci. 2005; 25(46):10598–606. doi:25/46/10598 [pii] 10.1523/JNEUROSCI.2990-05.2005. [PubMed: 16291932]

Kuo YM, Emmerling MR, Vigo-Pelfrey C, Kasunic TC, Kirkpatrick JB, Murdoch GH, Ball MJ, Roher AE. Water-soluble Abeta (N-40, N-42) oligomers in normal and Alzheimer disease brains. J Biol Chem. 1996; 271(8):4077–81. [PubMed: 8626743]

Kuo YM, Emmerling MR, Woods AS, Cotter RJ, Roher AE. Isolation, chemical characterization, and quantitation of A beta 3-pyroglutamyl peptide from neuritic plaques and vascular amyloid deposits. Biochem Biophys Res Commun. 1997; 237(1):188–91. doi:10.1006/bbrc.1997.7083. [PubMed: 9266855]

Kuperstein I, Broersen K, Benilova I, Rozenski J, Jonckheere W, Debulpaep M, Vandersteen A, Segers-Nolten I, Van Der Werf K, Subramaniam V, Braeken D, Callewaert G, Bartic C, D'Hooge R, Martins IC, Rousseau F, Schymkowitz J, De Strooper B. Neurotoxicity of Alzheimer's disease Abeta peptides is induced by small changes in the Abeta42 to Abeta40 ratio. The EMBO journal. 2010; 29(19):3408–20. doi:10.1038/emboj.2010.211. [PubMed: 20818335]

Langer F, Eisele YS, Fritschi SK, Staufenbiel M, Walker LC, Jucker M. Soluble Abeta seeds are potent inducers of cerebral beta-amyloid deposition. J Neurosci. 2011; 31(41):14488–95. doi:10.1523/JNEUROSCI.3088-11.2011. [PubMed: 21994365]

Lemere CA, Beierschmitt A, Iglesias M, Spooner ET, Bloom JK, Leverone JF, Zheng JB, Seabrook TJ, Louard D, Li D, Selkoe DJ, Palmour RM, Ervin FR. Alzheimer's disease abeta vaccine reduces central nervous system abeta levels in a non-human primate, the Caribbean vervet. Am J Pathol. 2004; 165(1):283–97. [PubMed: 15215183]

Lemere CA, Oh J, Stanish HA, Peng Y, Pepivani I, Fagan AM, Yamaguchi H, Westmoreland SV, Mansfield KG. Cerebral amyloid-beta protein accumulation with aging in cotton-top tamarins: a model of early Alzheimer's disease? Rejuvenation Res. 2008; 11(2):321–32. doi:10.1089/rej.2008.0677. [PubMed: 18341428]

Levine H 3rd, Walker LC. Molecular polymorphism of Abeta in Alzheimer's disease. Neurobiol Aging. 2010; 31(4):542–8. doi:S0197-4580(08)00182-6 [pii] 10.1016/j.neurobiolaging.2008.05.026. [PubMed: 18619711]

Lowenson JD, Clarke S, Roher AE. Chemical modifications of deposited amyloid-beta peptides. Methods in enzymology. 1999; 309:89–105. [PubMed: 10507019]

Lu JX, Qiang W, Yau WM, Schwieters CD, Meredith SC, Tycko R. Molecular structure of beta-amyloid fibrils in Alzheimer's disease brain tissue. Cell. 2013; 154(6):1257–68. doi:10.1016/j.cell.2013.08.035. [PubMed: 24034249]

Maeda J, Ji B, Irie T, Tomiyama T, Maruyama M, Okauchi T, Staufenbiel M, Iwata N, Ono M, Saido TC, Suzuki K, Mori H, Higuchi M, Suhara T. Longitudinal, quantitative assessment of amyloid, neuroinflammation, and anti-amyloid treatment in a living mouse model of Alzheimer's disease enabled by positron emission tomography. J Neurosci. 2007; 27(41):10957–68. doi:10.1523/JNEUROSCI.0673-07.2007. [PubMed: 17928437]

McGowan E, Pickford F, Kim J, Onstead L, Eriksen J, Yu C, Skipper L, Murphy MP, Beard J, Das P, Jansen K, Delucia M, Lin WL, Dolios G, Wang R, Eckman CB, Dickson DW, Hutton M, Hardy J, Golde T. Abeta42 is essential for parenchymal and vascular amyloid deposition in mice. Neuron. 2005; 47(2):191–9. doi:10.1016/j.neuron.2005.06.030. [PubMed: 16039562]

Mehta AK, Rosen RF, Childers WS, Gehman JD, Walker LC, Lynn DG. Context dependence of protein misfolding and structural strains in neurodegenerative diseases. Biopolymers. 2013; 100(6):722–30. doi:10.1002/bip.22283. [PubMed: 23893572]

Meyer-Luehmann M, Coomaraswamy J, Bolmont T, Kaeser S, Schaefer C, Kilger E, Neuenschwander A, Abramowski D, Frey P, Jaton AL, Vigouret J-M, Paganetti P, Walsh DM, Mathews PM, Ghiso J, Staufenbiel M, Walker LC, Jucker M. Exogenous induction of cerebral {beta}-amyloidogenesis is governed by agent and host. Science. 2006; 313(5794):1781–4. doi:10.1126/science.1131864. [PubMed: 16990547]

Miravalle L, Calero M, Takao M, Roher AE, Ghetti B, Vidal R. Amino-terminally truncated Abeta peptide species are the main component of cotton wool plaques. Biochemistry. 2005; 44(32):10810–21. doi:10.1021/bi0508237. [PubMed: 16086583]

Morales R, Bravo-Alegria J, Duran-Aniotz C, Soto C. Titration of biologically active amyloid-beta seeds in a transgenic mouse model of Alzheimer's disease. Sci Rep. 2015; 5:9349. doi:10.1038/srep09349. [PubMed: 25879692]

Morales R, Duran-Aniotz C, Castilla J, Estrada LD, Soto C. De novo induction of amyloid-beta deposition in vivo. Mol Psychiatry. 2012; 17(12):1347–53. doi:10.1038/mp.2011.120. [PubMed: 21968933]

Morawski M, Schilling S, Kreuzberger M, Waniek A, Jager C, Koch B, Cynis H, Kehlen A, Arendt T, Hartlage-Rubsamen M, Demuth HU, Rossner S. Glutaminyl cyclase in human cortex: correlation with (pGlu)-amyloid-beta load and cognitive decline in Alzheimer's disease. J Alzheimers Dis. 2014; 39(2):385–400. doi:10.3233/JAD-131535. [PubMed: 24164736]

Morrissette DA, Parachikova A, Green KN, LaFerla FM. Relevance of transgenic mouse models to human Alzheimer disease. J Biol Chem. 2009; 284(10):6033–7. doi:10.1074/jbc.R800030200. [PubMed: 18948253]

Murray MM, Bernstein SL, Nyugen V, Condron MM, Teplow DB, Bowers MT. Amyloid beta protein: Abeta40 inhibits Abeta42 oligomerization. J Am Chem Soc. 2009; 131(18):6316–7. doi:10.1021/ja8092604. [PubMed: 19385598]

Nelson PT, Alafuzoff I, Bigio EH, Bouras C, Braak H, Cairns NJ, Castellani RJ, Crain BJ, Davies P, Del Tredici K, Duyckaerts C, Frosch MP, Haroutunian V, Hof PR, Hulette CM, Hyman BT, Iwatsubo T, Jellinger KA, Jicha GA, Kovari E, Kukull WA, Leverenz JB, Love S, Mackenzie IR, Mann DM, Masliah E, McKee AC, Montine TJ, Morris JC, Schneider JA, Sonnen JA, Thal DR, Trojanowski JQ, Troncoso JC, Wisniewski T, Woltjer RL, Beach TG. Correlation of Alzheimer disease neuropathologic changes with cognitive status: a review of the literature. J Neuropathol Exp Neurol. 2012; 71(5):362–81. doi:10.1097/NEN.0b013e31825018f7. [PubMed: 22487856]

Nisbet RM, Polanco JC, Ittner LM, Gotz J. Tau aggregation and its interplay with amyloid-beta. Acta Neuropathol. 2015; 129(2):207–20. doi:10.1007/s00401-014-1371-2. [PubMed: 25492702]

Nussbaum JM, Schilling S, Cynis H, Silva A, Swanson E, Wangsanut T, Tayler K, Wiltgen B, Hatami A, Ronicke R, Reymann K, Hutter-Paier B, Alexandru A, Jagla W, Graubner S, Glabe CG, Demuth HU, Bloom GS. Prion-like behaviour and tau-dependent cytotoxicity of pyroglutamylated amyloid-beta. Nature. 2012; 485(7400):651–5. doi:10.1038/nature11060. [PubMed: 22660329]

Pauwels K, Williams TL, Morris KL, Jonckheere W, Vandersteen A, Kelly G, Schymkowitz J, Rousseau F, Pastore A, Serpell LC, Broersen K. Structural basis for increased toxicity of pathological abeta42:abeta40 ratios in Alzheimer disease. J Biol Chem. 2012; 287(8):5650–60. doi:10.1074/jbc.M111.264473. [PubMed: 22157754]

Perez SE, Raghanti MA, Hof PR, Kramer L, Ikonomovic MD, Lacor PN, Erwin JM, Sherwood CC, Mufson EJ. Alzheimer's disease pathology in the neocortex and hippocampus of the western lowland gorilla (Gorilla gorilla gorilla). J Comp Neurol. 2013; 521(18):4318–38. doi:10.1002/cne.23428. [PubMed: 23881733]

Petkova AT, Leapman RD, Guo Z, Yau WM, Mattson MP, Tycko R. Self-propagating, molecular-level polymorphism in Alzheimer's beta-amyloid fibrils. Science. 2005; 307(5707):262–5. [PubMed: 15653506]

Piccini A, Russo C, Gliozzi A, Relini A, Vitali A, Borghi R, Giliberto L, Armirotti A, D'Arrigo C, Bachi A, Cattaneo A, Canale C, Torrassa S, Saido TC, Markesbery W, Gambetti P, Tabaton M. Beta-Amyloid is different in normal aging and in Alzheimer disease. J Biol Chem. 2005; 34:186–92.

Pike CJ, Overman MJ, Cotman CW. Amino-terminal deletions enhance aggregation of beta-amyloid peptides in vitro. J Biol Chem. 1995; 270(41):23895–8. [PubMed: 7592576]

Portelius E, Andreasson U, Ringman JM, Buerger K, Daborg J, Buchhave P, Hansson O, Harmsen A, Gustavsson MK, Hanse E, Galasko D, Hampel H, Blennow K, Zetterberg H. Distinct cerebrospinal fluid amyloid beta peptide signatures in sporadic and PSEN1 A431E-associated familial Alzheimer's disease. Mol Neurodegener. 2010a; 5:2. doi:10.1186/1750-1326-5-2. [PubMed: 20145736]

Portelius E, Bogdanovic N, Gustavsson MK, Volkmann I, Brinkmalm G, Zetterberg H, Winblad B, Blennow K. Mass spectrometric characterization of brain amyloid beta isoform signatures in familial and sporadic Alzheimer's disease. Acta Neuropathol. 2010b; 120(2):185–93. doi:10.1007/s00401-010-0690-1. [PubMed: 20419305]

Portelius E, Lashley T, Westerlund A, Persson R, Fox NC, Blennow K, Revesz T, Zetterberg H. Brain amyloid-beta fragment signatures in pathological ageing and Alzheimer's disease by hybrid immunoprecipitation mass spectrometry. Neurodegener Dis. 2015; 15(1):50–7. doi: 10.1159/000369465. [PubMed: 25591542]

Portelius E, Zetterberg H, Andreasson U, Brinkmalm G, Andreasen N, Wallin A, Westman-Brinkmalm A, Blennow K. An Alzheimer's disease-specific beta-amyloid fragment signature in cerebrospinal fluid. Neurosci Lett. 2006; 409(3):215–9. doi:10.1016/j.neulet.2006.09.044. [PubMed: 17049739]

Querfurth HW, LaFerla FM. Alzheimer's disease. N Engl J Med. 2010; 362(4):329–44. doi:362/4/329 [pii] 10.1056/NEJMra0909142. [PubMed: 20107219]

Revesz T, Ghiso J, Lashley T, Plant G, Rostagno A, Frangione B, Holton JL. Cerebral amyloid angiopathies: a pathologic, biochemical, and genetic view. J Neuropathol Exp Neurol. 2003; 62(9): 885–98. [PubMed: 14533778]

Roher AE, Palmer KC, Yurewicz EC, Ball MJ, Greenberg BD. Morphological and biochemical analyses of amyloid plaque core proteins purified from Alzheimer disease brain tissue. J Neurochem. 1993; 61(5):1916–26. [PubMed: 8229002]

Rosen RF, Ciliax BJ, Wingo TS, Gearing M, Dooyema J, Lah JJ, Ghiso JA, LeVine H 3rd, Walker LC. Deficient high-affinity binding of Pittsburgh compound B in a case of Alzheimer's disease. Acta Neuropathol. 2010a; 119(2):221–33. doi:10.1007/s00401-009-0583-3. [PubMed: 19690877]

Rosen RF, Farberg AS, Gearing M, Dooyema J, P ML, Anderson DC, Davis-Turak J, Coppola G, Geschwind DH, Pare JF, Duong TQ, Hopkins WD, Preuss TM, Walker LC. Tauopathy with paired helical filaments in an aged chimpanzee. J Comp Neurol. 2008; 509(3):259–70. [PubMed: 18481275]

Rosen RF, Fritz JJ, Dooyema J, Cintron AF, Hamaguchi T, Lah JJ, LeVine H 3rd, Jucker M, Walker LC. Exogenous seeding of cerebral beta-amyloid deposition in betaAPP-transgenic rats. J Neurochem. 2012; 120(5):660–6. doi:10.1111/j.1471-4159.2011.07551.x. [PubMed: 22017494]

Rosen RF, Tomidokoro Y, Ghiso JA, Walker LC. SDS-PAGE/immunoblot detection of Abeta multimers in human cortical tissue homogenates using antigen-epitope retrieval. J Vis Exp. 2010b; (38) doi:10.3791/1916.

Rosen RF, Walker LC, Levine H 3rd. PIB binding in aged primate brain: enrichment of high-affinity sites in humans with Alzheimer's disease. Neurobiol Aging. 2011; 32(2):223–34. doi:10.1016/j.neurobiolaging.2009.02.011. [PubMed: 19329226]

Rufenacht P, Guntert A, Bohrmann B, Ducret A, Dobeli H. Quantification of the A beta peptide in Alzheimer's plaques by laser dissection microscopy combined with mass spectrometry. J Mass Spectrom. 2005; 40(2):193–201. doi:10.1002/jms.739. [PubMed: 15706631]

Sawamura N, Tamaoka A, Shoji S, Koo EH, Walker LC, Mori H. Characterization of amyloid beta protein species in cerebral amyloid angiopathy of a squirrel monkey by immunocytochemistry and enzyme-linked immunosorbent assay. Brain Res. 1997; 764(1-2):225–9. [PubMed: 9295214]

Schlenzig D, Manhart S, Cinar Y, Kleinschmidt M, Hause G, Willbold D, Funke SA, Schilling S, Demuth HU. Pyroglutamate formation influences solubility and amyloidogenicity of amyloid peptides. Biochemistry. 2009; 48(29):7072–8. doi:10.1021/bi900818a. [PubMed: 19518051]

Schlenzig D, Ronicke R, Cynis H, Ludwig HH, Scheel E, Reymann K, Saido T, Hause G, Schilling S, Demuth HU. N-Terminal pyroglutamate formation of Abeta38 and Abeta40 enforces oligomer formation and potency to disrupt hippocampal long-term potentiation. J Neurochem. 2012; 121(5): 774–84. doi:10.1111/j.1471-4159.2012.07707.x. [PubMed: 22375951]

Scholl M, Wall A, Thordardottir S, Ferreira D, Bogdanovic N, Langstrom B, Almkvist O, Graff C, Nordberg A. Low PiB PET retention in presence of pathologic CSF biomarkers in Arctic APP mutation carriers. Neurology. 2012; 79(3):229–36. doi:10.1212/WNL.0b013e31825fdf18. [PubMed: 22700814]

Selkoe, DJ. Biology of beta-amyloid precursor protein and the mechanism of Alzheimer disease.. In: Terry, RD.; R.K.; Bick, KL.; Sisodia, SS., editors. Alzheimer Disease. Lippincott Williams and Wilkins; Philadelphia: 1999. p. 293-310.

Selkoe DJ. Resolving controversies on the path to Alzheimer's therapeutics. Nat Med. 2011; 17(9): 1060–5. doi:10.1038/nm.2460. [PubMed: 21900936]

Selkoe DJ, Bell DS, Podlisny MB, Price DL, Cork LC. Conservation of brain amyloid proteins in aged mammals and humans with Alzheimer's disease. Science. 1987; 235(4791):873–7. [PubMed: 3544219]

Serdons K, Verduyckt T, Vanderghinste D, Cleynhens J, Borghgraef P, Vermaelen P, Terwinghe C, Van Leuven F, Van Laere K, Kung H, Bormans G, Verbruggen A. Synthesis of 18F-labelled 2-(4'-fluorophenyl)-1,3-benzothiazole and evaluation as amyloid imaging agent in comparison with [11C]PIB. Bioorg Med Chem Lett. 2009; 19(3):602–5. doi:10.1016/j.bmcl.2008.12.069. [PubMed: 19147351]

Simic G, Babic Leko M, Wray S, Harrington C, Delalle I, Jovanov-Milosevic N, Bazadona D, Buee L, de Silva R, Di Giovanni G, Wischik C, Hof PR. Tau Protein Hyperphosphorylation and Aggregation in Alzheimer's Disease and Other Tauopathies, and Possible Neuroprotective Strategies. Biomolecules. 2016; 6(1) doi:10.3390/biom6010006.

Sperling RA, Karlawish J, Johnson KA. Preclinical Alzheimer disease-the challenges ahead. Nat Rev Neurol. 2013; 9(1):54–8. doi:10.1038/nrneurol.2012.241. [PubMed: 23183885]

Stohr J, Condello C, Watts JC, Bloch L, Oehler A, Nick M, DeArmond SJ, Giles K, DeGrado WF, Prusiner SB. Distinct synthetic Abeta prion strains producing different amyloid deposits in bigenic mice. Proc Natl Acad Sci U S A. 2014; 111(28):10329–34. doi:10.1073/pnas.1408968111. [PubMed: 24982137]

Stohr J, Watts JC, Mensinger ZL, Oehler A, Grillo SK, DeArmond SJ, Prusiner SB, Giles K. Purified and synthetic Alzheimer's amyloid beta (Abeta) prions. Proc Natl Acad Sci U S A. 2012; 109(27):11025–30. doi:10.1073/pnas.1206555109. [PubMed: 22711819]

Struyfs H, Van Broeck B, Timmers M, Fransen E, Sleegers K, Van Broeckhoven C, De Deyn PP, Streffer JR, Mercken M, Engelborghs S. Diagnostic Accuracy of Cerebrospinal Fluid Amyloid-beta Isoforms for Early and Differential Dementia Diagnosis. J Alzheimers Dis. 2015; 45(3): 813–22. doi:10.3233/JAD-141986. [PubMed: 25633670]

Tekirian TL, Cole GM, Russell MJ, Yang F, Wekstein DR, Patel E, Snowdon DA, Markesbery WR, Geddes JW. Carboxy terminal of beta-amyloid deposits in aged human, canine, and polar bear brains. Neurobiol Aging. 1996; 17(2):249–57. [PubMed: 8744406]

Tekirian TL, Saido TC, Markesbery WR, Russell MJ, Wekstein DR, Patel E, Geddes JW. N-terminal heterogeneity of parenchymal and cerebrovascular Abeta deposits. J Neuropathol Exp Neurol. 1998; 57(1):76–94. [PubMed: 9600199]

Tekirian TL, Yang AY, Glabe C, Geddes JW. Toxicity of pyroglutaminated amyloid beta-peptides 3(pE)-40 and -42 is similar to that of A beta1-40 and -42. J Neurochem. 1999; 73(4):1584–9. [PubMed: 10501204]

Tomidokoro Y, Lashley T, Rostagno A, Neubert TA, Bojsen-Moller M, Braendgaard H, Plant G, Holton J, Frangione B, Revesz T, Ghiso J. Familial Danish dementia: co-existence of Danish and Alzheimer amyloid subunits (ADan AND A{beta}) in the absence of compact plaques. J Biol Chem. 2005; 280(44):36883–94. doi:10.1074/jbc.M504038200. [PubMed: 16091362]

Toyama H, Ye D, Ichise M, Liow JS, Cai L, Jacobowitz D, Musachio JL, Hong J, Crescenzo M, Tipre D, Lu JQ, Zoghbi S, Vines DC, Seidel J, Katada K, Green MV, Pike VW, Cohen RM, Innis RB. PET imaging of brain with the beta-amyloid probe, [11C]6-OH-BTA-1, in a transgenic mouse model of Alzheimer's disease. European journal of nuclear medicine and molecular imaging. 2005; 32(5):593–600. [PubMed: 15791432]

Walker LC, Callahan MJ, Bian F, Durham RA, Roher AE, Lipinski WJ. Exogenous induction of cerebral beta-amyloidosis in betaAPP-transgenic mice. Peptides. 2002; 23(7):1241–7. [PubMed: 12128081]

Walker, LC.; Cork, LC. The neurobiology of aging in nonhuman primates.. In: Terry, RD., editor. Alzheimer Disease. Lippincott Williams and Wilkins; Philadelphia, PA: 1999. p. 233-43.

Walker LC, Kitt CA, Schwam E, Buckwald B, Garcia F, Sepinwall J, Price DL. Senile plaques in aged squirrel monkeys. Neurobiol Aging. 1987; 8(4):291–6. [PubMed: 3306432]

Walker LC, Masters C, Beyreuther K, Price DL. Amyloid in the brains of aged squirrel monkeys. Acta Neuropathol (Berl). 1990; 80(4):381–7. [PubMed: 2239150]

Walker LC, Pahnke J, Madauss M, Vogelgesang S, Pahnke A, Herbst EW, Stausske D, Walther R, Kessler C, Warzok RW. Apolipoprotein E4 promotes the early deposition of Abeta42 and then Abeta40 in the elderly. Acta Neuropathol. 2000; 100(1):36–42. [PubMed: 10912918]

Watt AD, Perez KA, Rembach A, Sherrat NA, Hung LW, Johanssen T, McLean CA, Kok WM, Hutton CA, Fodero-Tavoletti M, Masters CL, Villemagne VL, Barnham KJ. Oligomers, fact or artefact? SDS-PAGE induces dimerization of beta-amyloid in human brain samples. Acta Neuropathol. 2013; 125(4):549–64. doi:10.1007/s00401-013-1083-z. [PubMed: 23354835]

Watts JC, Condello C, Stohr J, Oehler A, Lee J, DeArmond SJ, Lannfelt L, Ingelsson M, Giles K, Prusiner SB. Serial propagation of distinct strains of Abeta prions from Alzheimer's disease patients. Proc Natl Acad Sci U S A. 2014; 111(28):10323–8. doi:10.1073/pnas.1408900111. [PubMed: 24982139]

Watts JC, Giles K, Grillo SK, Lemus A, DeArmond SJ, Prusiner SB. Bioluminescence imaging of Abeta deposition in bigenic mouse models of Alzheimer's disease. Proc Natl Acad Sci U S A. 2011; 108(6):2528–33. doi:10.1073/pnas.1019034108. [PubMed: 21262831]

Wilhelmus MM, de Waal RM, Verbeek MM. Heat shock proteins and amateur chaperones in amyloid-Beta accumulation and clearance in Alzheimer's disease. Mol Neurobiol. 2007; 35(3):203–16. [PubMed: 17917109]

Ye L, Fritschi SK, Schelle J, Obermuller U, Degenhardt K, Kaeser SA, Eisele YS, Walker LC, Baumann F, Staufenbiel M, Jucker M. Persistence of Abeta seeds in APP null mouse brain. Nat Neurosci. 2015a; 18(11):1559–61. doi:10.1038/nn.4117. [PubMed: 26352792]

Ye L, Hamaguchi T, Fritschi SK, Eisele YS, Obermuller U, Jucker M, Walker LC. Progression of Seed-Induced Abeta Deposition within the Limbic Connectome. Brain Pathol. 2015b; 25(6):743–52. doi:10.1111/bpa.12252. [PubMed: 25677332]

Highlights

- Aβ peptide fragments are similar in Alzheimer's disease and aged monkeys
- Aggregated Aβ from aged monkeys induces Aβ deposition in transgenic mice
- Simian Aβ has distinctive epitope exposure and few high-affinity PiB binding sites
- Molecular conformational variation may influence the pathogenicity of aggregated Aβ

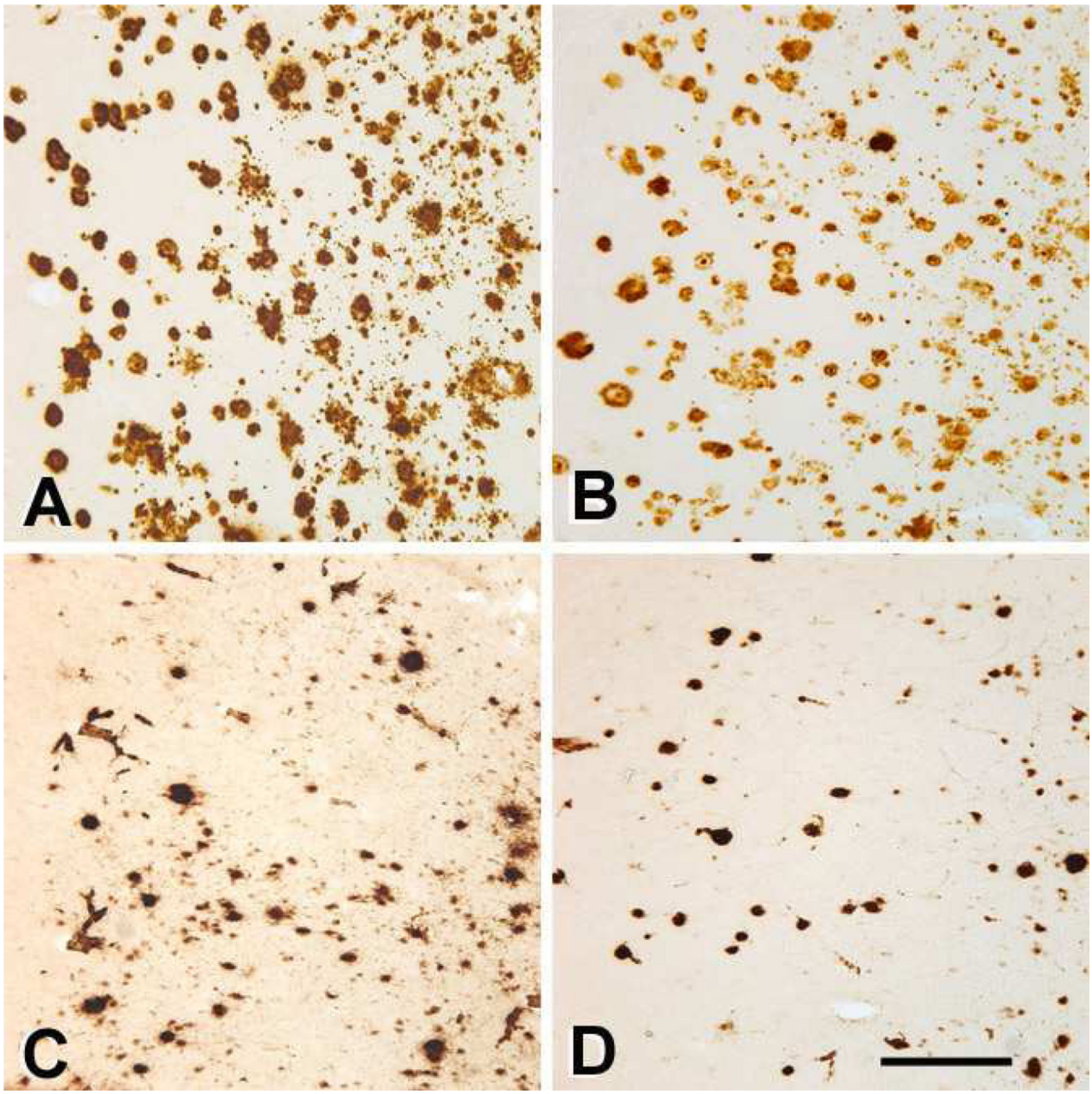

Figure 1. Aβ deposition in the temporal neocortices of a human with AD (AD2; A, B) and an aged squirrel monkey (Ss4; C, D)

Panels A and C show immunoreactivity to antibody 6E10 to unmodified Aβ residues 3-8, and panels B and D show immunoreactivity to antibody 8E1 to Aβ[$_{\text{pyroglutamate}}$3]-x. Scale bar = 300μm for all panels.

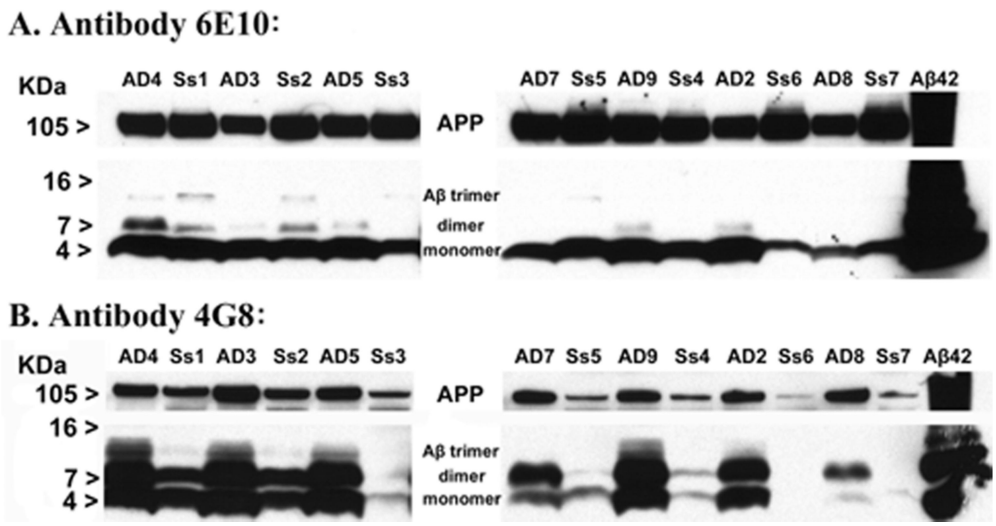

Figure 2. Western blot analysis of multimeric Aβ distribution in AD and aged squirrel monkey temporal neocortices

Clarified temporal cortical homogenates (low-speed supernatants) from 7 end-stage AD cases and 7 aged squirrel monkeys, normalized to 60 μg total protein, were electrophoretically separated in SDS by molecular weight on a Tris-Tricine 10-20% gel and immunoblotted with anti-Aβ antibodies 6E10 (top) and 4G8 (bottom). (A) Immunoblotting with antibody 6E10 revealed strong bands migrating at approximately 4 kDa in all extracts, which correspond to monomeric Aβ40 and Aβ42. Dimeric and trimeric Aβ species were also detected in some AD and squirrel monkey samples, particularly in the cases shown to have higher levels of Aβ by ELISA (see Table 1). (B) The 4G8 antibody detected strong bands of Aβ monomers in nearly all AD and squirrel monkey extracts. 4G8-immunoreactive bands corresponding to Aβ dimers and trimers were substantially stronger in most AD samples than in squirrel monkeys with comparable levels of total Aβ as shown by ELISA. Both antibodies bound to a band migrating around 105KDa, or full-length APP, in all samples. In the last lane, 100ng of fibrillar synthetic Aβ42 was run as a positive control. AD: Human Alzheimer's disease cases, Ss: Squirrel monkey (*Saimiri sciureus*); each lane represents a separate case.

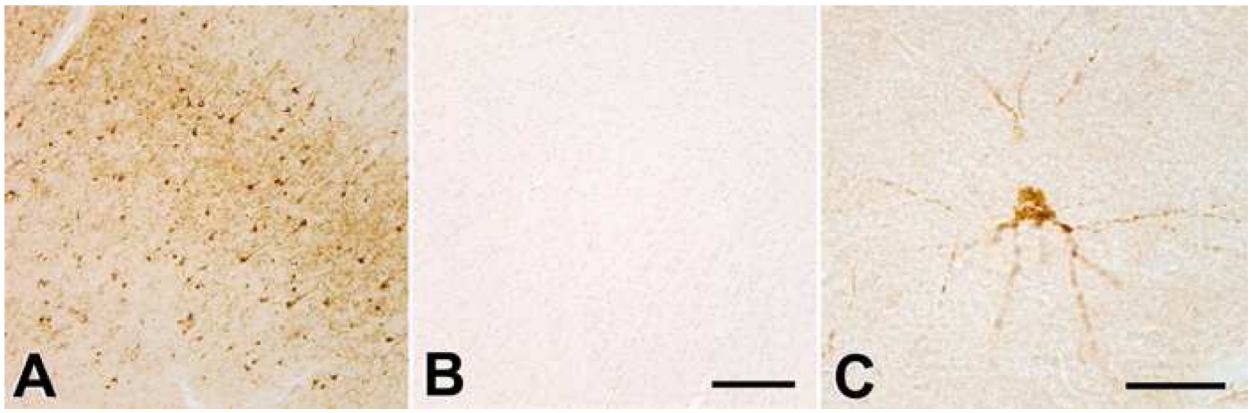

Figure 3. Tau-immunostaining in the neocortices of patient with AD (AD2; A) and a 23-year old squirrel monkey (Ss4; B, C)

Panels A and B depict the superior temporal gyrus stained using antibody MC1 to aggregated tau; note the general absence of immunoreactive neurons in the aged squirrel monkey (B) (the cortical surface is to the upper right in both panels). Panel C depicts a rare cortical cell that is immunoreactive with antibody CP13 to hyperphosphorylated tau in squirrel monkey Ss4. Occasional tau-immunoreactive neurons and neurites occur in senescent squirrel monkeys, but AD-like tauopathy has not yet been demonstrated in any aged monkey. Scale bars = 250μm in B (applies also to A) and 50μm in C.

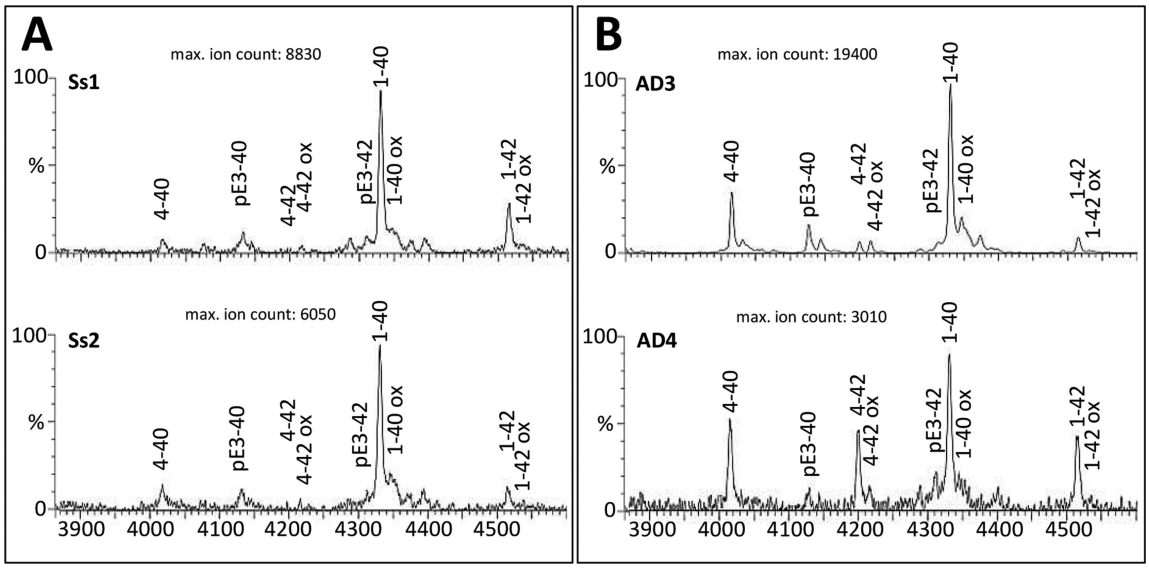

C

	EXPERIMENTAL MASS (M + H⁺)								
Tissue \ Aβ species	4-40	pE3-40	4-42	4-42ox	pE3-42	1-40	1-40ox	1-42	1-42ox
AD2 occ	4016.8		4199.2			4330.2		4515.0	
AD3 occ	4016.7		4200.7		4311.7	4330.8		4515.0	
AD3 tem	4015.7	4126.6	4200.4	4216.2		4330.8	4346.6	4515.2	
AD4 occ	4015.6	4128.0	4200.9	4216.6	4311.5	4330.9	4345.1	4514.3	
AD4 tem	4014.8	4125.5	4200.8	4215.1		4330.0	4346.4	4514.4	
AD5 occ	4016.5	4127.2	4200.9	4216.5	4310.6	4330.1	4346.7	4515.6	
AD6 occ			4200.5			4329.8		4515.6	
Ss1 occ	4017.8				4312.0	4330.8		4516.0	4531.4
Ss1 tem				4214.7		4330.0		4514.8	
Ss2 occ	4017.2				4312.9	4331.0	4345.6	4514.0	
Ss2 tem	4015.6	4125.6		4214.7		4329.7	4346.0	4514.4	
Ss3 occ	4017.3				4312.7	4330.4		4516.4	4531.9
Ss3 tem		4125.2				4331.0	4345.9	4516.0	
M+H⁺ (EXPECTED)	4015.6	4126.7	4199.8	4215.8	4310.9	4330.9	4346.9	4515.1	4531.1

Figure 4. MALDI-TOF mass spectrometry analysis of insoluble Aβ peptides in AD and aged squirrel monkey neocortices

Panel A: Aβ spectra obtained from occipital cortical extracts of two aged-squirrel monkey specimens, Ss1 (top) and Ss2 (bottom). **Panel B**: Aβ spectra obtained from temporal and occipital extracts of two AD patients (AD3, top; AD4, bottom). Labeled peaks correspond to full-length, truncated, or post-translationally-modified Aβ peptides. **Panel C**: Comparative list of theoretical and experimental *m/z* values for all AD and monkey samples tested As a

whole, the spectrometric pattern of Aβ peptides in aged squirrel monkeys was similar to that of the AD group.

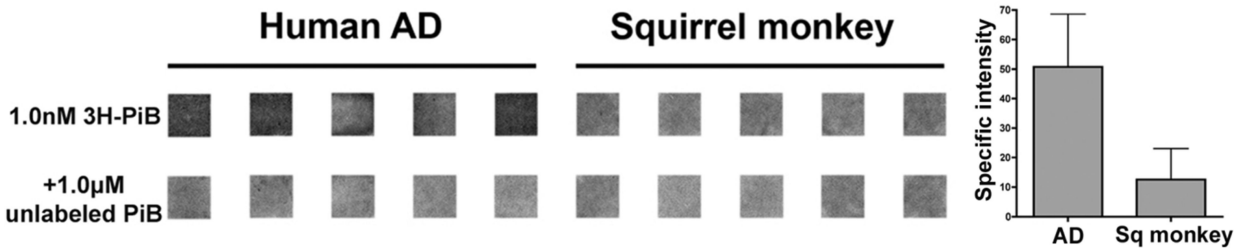

Figure 5. Radiospotblot detection of high-affinity ^{3}H-PiB binding sites in AD and aged squirrel monkey neocortices

Aβ-rich temporal cortical extracts (derived from 300μg wet tissue) from AD and squirrel monkey cases (n=5/group) were analyzed by ^{3}H-PiB radiospotblot. In the top row, dried extracts were incubated with 1.0nM ^{3}H-PiB. Samples in the bottom row were co-incubated with 1.0nM ^{3}H-PiB and 1.0μM unlabeled PiB to determine levels of nonspecific ligand binding. Shown are identical regions of interest from a single film exposure. Darker signal indicates the presence of specifically bound radioligand, quantified at right.

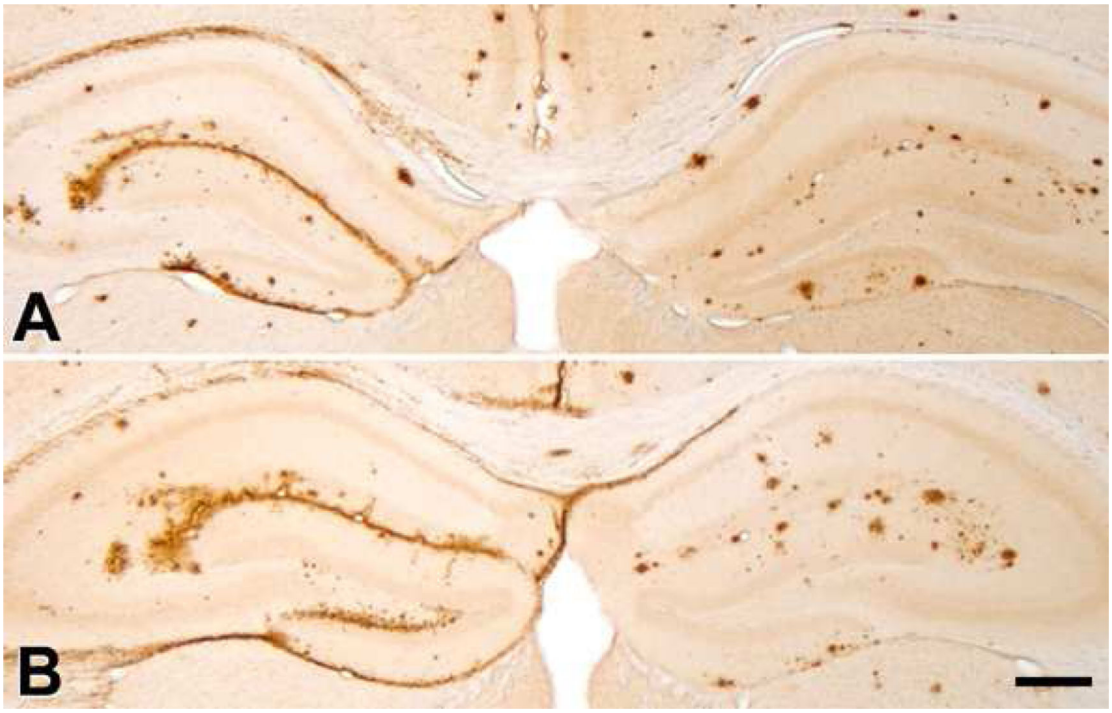

Figure 6. Seeding of Aβ deposition in APP/PS1 mouse hippocampi by Aβ-rich cortical extracts from an AD case and an aged squirrel monkey

The mice were injected unilaterally (left) at 13-14 weeks of age with 2.5μl of clarified 10% brain extract from human case AD4 (**A**) or an aged squirrel monkey (Ss1, **B**). The contralateral hemisphere (right) was injected with PBS as a sham control. The brains were analyzed after a 22 week incubation period, when the mice were ~8 months of age; at this age, endogenous, mostly spherical plaques have begun to form in these APP/PS1 mice. Note the re-distribution and heavy deposition of Aβ along the hippocampal fissure, subpial zone, and in the corpus callosum of both AD- and squirrel monkey-seeded hippocampi. Antibody R398 to Aβ42. Immunostaining of the seeded deposits was similar for antibodies to Aβ40 and Aβ42 in both the AD-seeded and squirrel monkey-seeded host mice. Scale bar = 300μm for both panels.

Neurobiol Aging. Author manuscript; available in PMC 2017 August 01.

Table 1

[*] Subject characteristics and insoluble Aβ levels.

Group	Case	$\Delta_{Age(y)}$	Sex	$\S_{PMI(h)}$	$\#_{Braak\ Stage}$	$^{**}ApoE$	AβTC	(42:40)	AβOC	(42:40)
Human ND	ND1	40	m	31	Braak 0	3/4	1	(nc)	1	(nc)
	ND2	57	f	17	Braak 0	3/3	bd	(nc)	bd	(nc)
	ND3	75	f	6	Braak 0	3/3	bd	(nc)	1	(nc)
Human AD	AD1[T,O]	57	f	20	Braak V/VI	3/4	86	(27.7)	213	(105.5)
	AD2[O,^]	87	f	6	Braak V/VI	3/4	225	(27.1)	187	(16.0)
	AD3[T,O]	75	f	12	Braak V/VI	4/4	160	(1.6)	192	(37.4)
	AD4[T,O,^]	61	m	5.5	Braak V/VI	3/4	215	(4.4)	313	(19.9)
	AD5[O]	91	f	2.5	Braak V/VI	3/4	214	(10.9)	202	(19.1)
	AD6[O]	81	f	2	Braak >IV	3/3	146	(146.0)	60	(nc)
	AD7	61	m	4	Braak V/VI	3/4	628	(1.3)	na	
	AD8	84	m	4.5	Braak VI	3/4	160	(39.0)	na	
	AD9	64	f	4.5	Braak VI	3/4	449	(111.3)	na	
Squirrel monkey	Ss1[T,O,^]	21	m	1			597	(0.6)	1014	(1.6)
	Ss2[T,O,^]	20	m	1			750	(0.5)	1629	(0.5)
	Ss3[T,O]	17	m	1			99	(11.4)	176	(174.0)
	Ss4	23	f	<3			337	(16.7)	396	(14.2)
	Ss5	17	m	1			360	(119.0)	221	(4.1)
	Ss6	15	m	1			52	(nc)	2	(nc)
	Ss7[O]	14	m	1			na	na	na	na

AD – Alzheimer's disease; ND – non-demented; Ss – *Saimiri sciureus* (squirrel monkeys)

AβTC, AβOC – fmol total insoluble Aβ (Aβ42 + Aβ40) per 100μg tissue in temporal neocortex and occipital neocortex, respectively

(42:40) – ratio of insoluble Aβ42:Aβ40 in each brain region

na: not available

nc: not calculable

bd: below detection

* Modified from Rosen et al. (2011)

Δ Age(y): Age (years)

§ PMI(h): Postmortem interval (hours)

** ApoE: Apolipoprotein E genotype [note: all nonhuman primates analyzed to date are apoE4/4 according to human nomenclature (Morelli, et al., 1996)]

T Temporal cortex samples used for MALDI-TOF experiments

O Occipital cortex samples used for MALDI-TOF experiments

^ Samples used for *in vivo* seeding experiments

Braak and Braak (1991)(Braak and Braak, 1991)